Tissue distribution of an anti-TB drug, TBA-354 in rats *via* mass spectrometric investigations

by

Sphamandla Ntshangase

2016

Tissue distribution of an anti-TB drug, TBA-354 in rats *via* mass spectrometric investigations

Sphamandla Ntshangase

2016

A thesis submitted to the School of Health Sciences, College of Health Science, University of KwaZulu-Natal, Westville, for the degree of Master of Medical Science. This is the thesis in which the chapters are written as a set of discrete research publications that have followed the Journal of Antimicrobial Chemotherapy format with an overall introduction and final summary. Typically, these chapters will have been published in internationally recognized, peer-reviewed journals.

This is to certify that the contents of this thesis are the original research work of Mr. Sphamandla Ntshangase, carried out under our supervision at the Catalysis and Peptide Research Unit, Westville campus, University of KwaZulu-Natal, Durban, South Africa and Biomedical Resource Unit, Westville campus, University of KwaZulu - Natal, Durban, South Africa.

Supervisor:

Signed: _____Name: Prof. T Govender Date: _____

Co-Supervisor:

Signed: _____Name: Prof. H G Kruger Date: _____

Co-Supervisor:

Signed: _____Name: Dr. G.E.M Maguire Date: _____

Abstract

Tuberculosis (TB) (TB) is one of the most well-recognized ancient human diseases in the history of mankind and it remains the major cause of human death amongst the transmittable diseases despite the use of antitubercular antibiotics. TB is caused by a pathogenic bacterium known as *Mycobacterium tuberculosis* (*M.tb*). The *M.tb* bacteria primary site of infection is the human lungs (resulting in pulmonary TB) but it can also affect other body parts (extrapulmonary TB) such as the bones, central nervous system (CNS), liver and many more others. Present-day TB research is focused on the development of more effective anti-TB drugs that can help shorten the treatment period. One of the major set-backs in TB drug development is to find the balance between the potential drug's side effects and its activity.

The present demonstrates the potential of liquid chromatography-tandem mass spectrometry (LC-MS/MS) and matrix-assisted laser desorption/ionization (MALDI) mass spectrometry imaging (MSI) techniques in the evaluation of the fundamental *in-vivo* pharmacokinetics and tissue distribution properties of a bicyclic nitroimidazole derivative, TBA-354. This drug is recognized to have an excellent activity against *M.tb* strains but also known to have mild signs of neurotoxicity. The use of MSI in this study shows the exact localization and accumulation of the drug in the brain, providing evidence as to why it showed certain neurotoxic signs during clinical trials. The study was conducted on healthy female Sprague-Dawley rats by administering 20 mg/kg of the drug, *via* an intraperitoneal (i.p.) route. After dosing the biological samples (plasma, lungs and brain) were collected at different time points for analysis. A validated LC-MS/MS method was used to quantify TBA-354 in rat plasma, lung and brain homogenate samples. LC-MS/MS cannot provide enough information regarding the drug localization and where it accumulates in the brain, therefore, MSI was then used to study the accumulation of the drug in different regions of the brain.

As per LC-MS/MS results, the drug showed significant pharmacokinetic and distribution properties in the rat model with the highest levels in plasma compared to lung and brain. MALDI-MSI results showed that the drug was effectively able cross the blood-brain barrier (BBB) resulting in toxic accumulation in the neocortical regions of the brain. This study has proven the efficacy of MSI as a suitable analytical technique that can be used in future preclinical studies to evaluate the neurotoxicity of drugs targeting the brain, thus minimizing possible side effects.

Declaration 1 - plagiarism

I, Mr. Sphamandla Ntshangase declare that

- The research reported in this thesis, except where otherwise indicated, and is my original research.

1. This thesis has not been submitted for any degree or examination at any other university.

2. This thesis does not contain other persons' data, pictures, graphs or other information unless specifically acknowledged as being sourced from other persons.

3. This thesis does not contain other person's writing unless specifically acknowledged as being sourced from other researchers. Where other written sources have been quoted, then:

    a. Their words have been re-written but the general information attributed to them has been referenced

    b. Where their exact words have been used, then their writing has been placed in italics and inside quotation marks and referenced.

    c. This thesis does not contain text, graphics or tables copied and pasted from the internet, unless specifically acknowledged, and the source being detailed in the thesis and in the references sections.

Signed

_____

Declaration 2 - List of publications

1. Sphamandla Ntshangase, Sooraj Baijnath, Adeola Shobo, Sanil D. Singh, Glenn Maguire, Gert Kruger, Per Arvidsson, Tricia Naicker, Thavendran Govender. The downfall of TBA-354 – investigating its neurotoxicity in the brain using mass spectrometry. **Journal of Antimicrobial Chemotherapy. Submitted 2016.**

Acknowledgements

I would like to thank the following people, institutions and departments;

- My supervisors Prof. Thavendran Govender, Prof. Gert Kruger, Dr. Tricia Naicker, Dr. Glenn Maguire for their motivation and guidance throughout my research.

- My co-supervisors, Mr. Sooraj Baijnath and Dr. Adeola Shobo, whenever I had a question about my research or writing there were always there to help.

- School of Health Sciences at the University of KwaZulu-Natal and National Research Foundation (NRF) for their financial support.

- Finally, I would like to express my deep gratitude to my family, especially my sister Nontobeko Mnguni and to the whole CPRU team for providing me with the support and constant motivations during the study. This achievement would have been impossible without them. Thank you.

Contents

List of figures

List of tables

List of abbreviations

% RSD	: percentage relative standard deviation
ACN	: acetonitrile
APCI	: atmospheric pressure chemical ionization
AREC	: Animal Research Ethics Committee
ATP	: adenosine triphosphate
ATR	: antiretroviral therapy
AUC	: area under the concentration vs time curve
AUC_{0-t}	: AUC from 0 hours to the time of the last measurable concentration
BBB	: blood-brain barrier
CHCA	: α-cycno-4-hydroxy-cinnamic acid
CI	: chemical ionization
C_{max}	: maximum concentration occurring in a profile
CNS	: central nervous system
CPRU	: Catalysis and Peptide Research Unit
DMSO	: dimethyl sulfoxide
EI	: electron ionization
EMA	: European Medicines Agency
EPTB	: extrapulmonary tuberculosis
ESI	: electrospray ionization
FA	: formic acid
FAB	: fast atom bombardment
FT-ICR	: Fourier transform ion cyclotron resonance
GC	: gas chromatography
HIV	: human immunodeficiency virus
HQC	: high quality control

i.p.	: intraperitoneal
IS	: internal standard
ITO	: indium titanium oxide
K3-EDTA	: tri-potassium ethylenediaminetetraacetic acid
LC	: liquid chromatography
LC-MS/MS	: liquid chromatography-tandem mass spectrometry
LLOQ	: lower limit of quantification
LQC	: low quality control
M.tb	: mycobacterium tuberculosis
m/z	: mass-to-charge ratio
MALDI	: matrix-assisted laser desorption/ionization
MALDI-MS	: matrix-assisted laser desorption/ionization-mass spectrometry
MALDI-MSI	: matrix-assisted laser desorption/ionization-mass spectrometry imaging
MDR-TB	: multi-drug resistant tuberculosis
MeOH	: methanol
MIC	: minimum inhibitory concentration
MQC	: mid quality control
MRI	: magnetic resonance imaging
MRM	: multiple reaction monitoring
MS	: mass spectrometry
MSI	: mass spectrometry imaging
PET	: positron emission tomography
PK	: pharmacokinetic
PTB	: pulmonary tuberculosis
QC	: quality control
RT	: retention time

S/N	: signal-to-noise
SA	: South Africa
SD	: standard deviation
SPE	: solid-phase extraction
STD	: sexually transmitted disease
$t_{1/2}$	: terminal half-life
TB	: tuberculosis
TBM	: tuberculous meningitis
T_{max}	: time of maximum concentration
TOF	: time-of-flight
TOF-MS	: time-of-flight mass spectrometry
UKZN	: University of KwaZulu-Natal
USFDA	: United States Food and Drug Administration
UV	: ultraviolet
WHO	: World Health Organization
XDR-TB	: extensively drug-resistant tuberculosis

Chapter 1

Introduction, aims and objectives

1.1. Introduction

This chapter provides a general background on tuberculosis (TB), nitroimidazole drugs and their activities against TB. It also explains the basic principles of liquid chromatography-tandem mass spectrometry (LC-MS/MS) and matrix-assisted laser desorption/ionization-mass spectrometry imaging (MALDI-MSI) techniques and their applications in pre-clinical biomedical research.

1.1.1. Background

TB is one of the ancient infectious diseases well-known to mankind. It is caused by *Mycobacterium tuberculosis* (*M.tb*) bacteria and still remains a major global health problem [1]. According to statistics generated by the World Health Organization (WHO), 10.4 million TB cases occurred in 2015 worldwide [2]. TB is predominant to people living with the human immunodeficiency virus (HIV) across the world, mainly in sub-Saharan African countries [3]. South Africa (SA) is among the countries considered to be worst affected (**Figure 1.1**) [2, 4]. The synergistic relationship between HIV and TB is a serious global health problem [5]. HIV-positive individuals are more susceptible to TB infection since they have low CD4 cell counts [6]. In many cases, TB is a primary sign that a patient living with it is also HIV-positive [7]. WHO claims that 1.4 million people died of TB in 2015, of which 0.4 million of them were HIV-positive [2], regardless of the antiretroviral therapy (ATR) being universally commended. Medical scientists are still unsure about the prescription of ART to patients who are co-infected by HIV and TB because they are concerned about possible overlaps on drug toxicity, immune recovery syndrome and drug to drug interactions [3, 8].

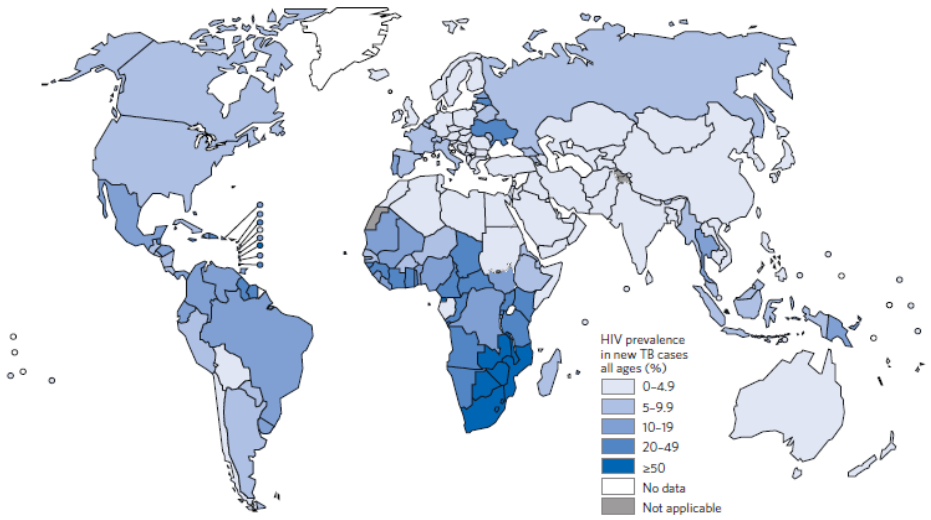

Figure 1.1. Global WHO predictions (2015) on HIV prevalence in recent TB incidences (%) [2].

The first anti-TB drugs were introduced in the early 1950s which include isoniazid [9], streptomycin [10] and para-aminosalicylic acid [11, 12]. Rifampicin is the most effective first-line antitubercular drug and was approved for TB chemotherapy in the 1960s [2]. Currently, the recommended treatment of drug-susceptible TB takes a period of six months and it is comprised of four first-line drugs: rifampicin, pyrazinamide, ethambutol and isoniazid [13]. The treatment of TB is often a challenge since the *M.tb* bacteria has the ability to remain active in the host for a prolonged period [14]. The *M.tb* bacteria has evolved to a stage of being multi-drug resistant (MDR-TB) [15, 16] and extensively drug resistant (XDR-TB) [17] and is often unsusceptible to all fluoroquinolone drugs and to either one of the second-line anti-TB medications (kanamycin, amikacin, and capreomycin) [18]. The resistance of *M.tb* results in an increased number of deaths per year. Another main issue towards high mortality is the prolonged period of TB chemotherapy which is required to completely cure the disease [19]. There is a necessity to develop effective anti-TB drugs with advanced mechanisms of action, specifically for use in shorter treatment. Several new anti-TB drug candidates in clinical development have demonstrated great potency against TB in animal models and clinical trials [20].

The most common form of TB is pulmonary TB (PTB) [21], but extrapulmonary TB (EPTB) [22] also accounts for a significant increase of all cases reported across the world [23, 24]. Amongst the HIV-negative people, EPTB mainly affects children and women [25]. Tuberculous meningitis (TBM) [26, 27] also caused by *M.tb*, is the most challenging and dangerous of all forms of TB [28]. Nearly half of TBM cases result in mortality or severe disabilities if not treated immediately [29]. This highlights the need for researchers to develop new anti-TB drugs that can effectively penetrate the central nervous system (CNS), get into the cerebrospinal fluid and cross the blood-brain barrier (BBB).

With drug resistance being the main issue, there are some setbacks in TB drug development studies. The anti-TB drug candidates under development [30] and the first-line drugs either have adverse side effects such as toxicity or have poor activity against TB. The BBB is the main route for the entry of most important molecules into the brain and it is also a formidable barrier that prevents many neurotoxic molecules from entering the brain. Only a few studies on the neurotoxic potential of some anti-TB drugs exist [31-33].

1.1.2. Nitroimidazole drugs

Nitroimidazole drugs were discovered in the mid-1950s at Rhone-Poulenc (French chemical and pharmaceutical company launched in 1928) during the search for drugs active against the sexually transmitted disease trichomoniasis (caused by a protozoan parasite called *Trichomonas vaginitis*) with metronidazole [34, 35] being the first of nitroimidazole drugs to be discovered [36]. The metronidazole drugs have also been used to treat diseases caused by either Gram-negative or Gram-positive bacteria.

Those include the *Bacteroides fragilis* which is a causative agent for peritoneal infections and *Clostridium difficile*, which causes pseudomembranous colitis [37]. Metronidazoles are also used in the treatment of stomach ulcers caused by *Helicobacter pylori* [38]. The second discovery was 2-nitroimidazole which was found to be active against *Trichomonas vaginitis* a mobile parasitic protozoan wich causes sexually transmitted disease (STD), trichomoniasis [39].

Nitroimidazoles are a class of compounds that most of them have been found to be active against drug-resistant TB [40]. Current drug development for TB has been fixated to the usage of the nitroimidazole class of compounds since they have an unusual mode of action and have reduced chances of becoming resistant [41]. The nitroimidazole drugs that have shown activity against TB in the past are illustrated in **Figure 1.2**.

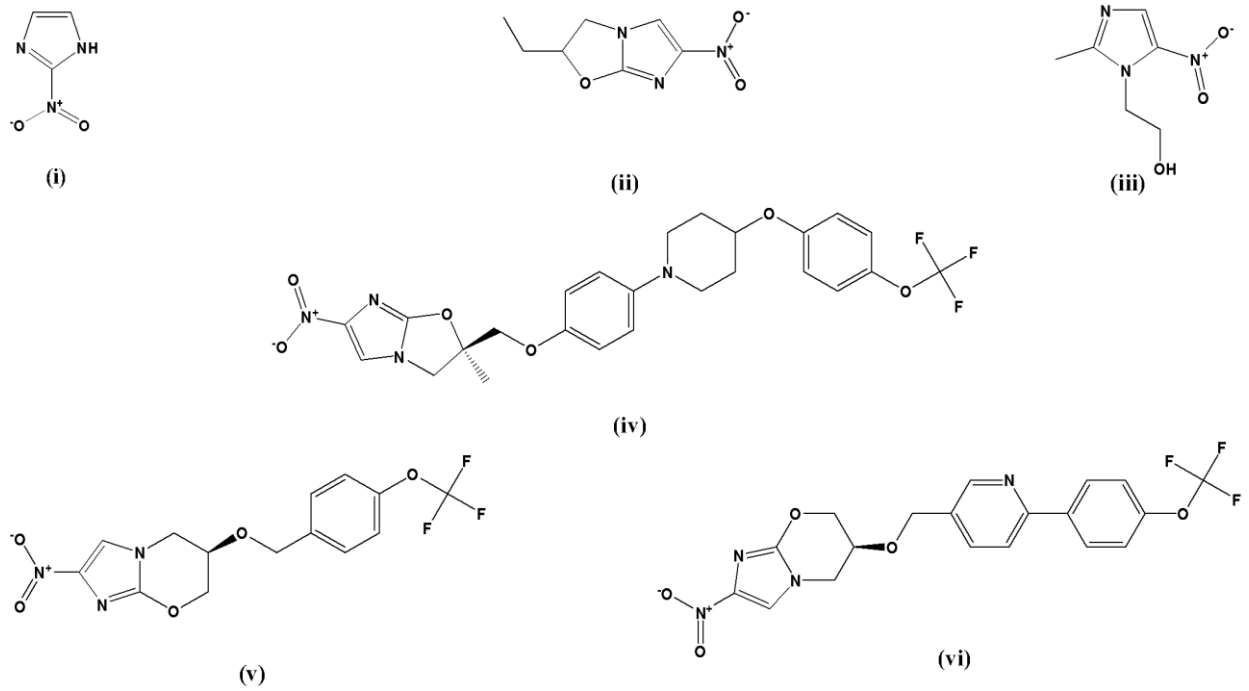

Figure 1.2. Anti-tubercular nitroimidazole drugs: (i) 2-nitroimidazole [39], (ii) CGI-17341 [42], (iii) metronidazole [39], (iv) delamanid [43], (v) pretomanid (PA-824) [44] and (vi) TBA-354 [40].

Previous stuidies have shown that CGI-17341 has good *in-vitro* activity against MDR-TB [45]. Unfortunately, CGI-17341 was found to be mutagenic, which resulted in the discontinuation of further investigations on TB, but further optimizations led to the discovery of other nitroimidazole derivatives; pretomanid (PA-824), TBA-354 and delamanid [40]. Pretomanid was developed by the TB alliance [46] and has the potential for TB therapy because of its unusual mechanism of action [40]. Moreover, the drug was found to be non-mutagenic and it is one of the most promising anti-TB drugs in the present TB drug

pipeline [47]. Pretomanid acts as a pro-drug in the process and the aerobic mode action seem to cause the suppression of mycolic acid biosynthesis by the cell wall through a yet unidentified mechanism [48]. Studies based on microarray analysis [14, 49] for the elucidation of pretomanid's mechanism of action showed that there were mixed and complex effects on the genes that are reactive to both the cell wall inhibition and respiratory chain toxication [50]. The nitro group plays an important role in the anaerobic killing of *M.tb* [50]. The nitro group from pretomanid is released inside the mycobacterial cells, it then reacts rapidly with the cytochrome oxidase preventing an electron flow and adenosine triphosphate (ATP) homeostasis under hypoxic static conditions [50]. Some of the nitroimidazole compounds recently studied were non-mutagenic and demonstrated bactericidal activity towards the replicating and static *M.tb*, which also includes the MDR-TB [20]. The United States Food and Drug Administration (USFDA) has accepted only two antitubercular drugs (delamanid and bedaquiline) for MDR-TB treatment in the last 40 years [51, 52].

TBA-354 has a mechanism of action comparable to that of pretomanid and it is claimed to be even more effective than pretomanid with the potency of five to ten times greater [40, 53]. TBA-354 has been tested in both *in-vivo* and *in-vitro* activity against *M.tb*. The *in-vitro* and *in-vivo* investigations in mice demonstrated that TBA-354 has the highest bioavailability and a longer elimination half-life when compared to other anti-TB nitroimidazole derivatives currently under clinical development[40].

Toxicity of anti-TB drug candidates under development is one of the major setbacks in TB research. Recently, an unlucky incident occurred during the TB clinical trials where TBA-354 showed signs of neurotoxicity based on the findings gathered by the TB alliance [47]. As a result, further clinical trials involving TBA-354 has been discontinued (11 March 2016) [47, 54]. Even though TBA-354 development has been stopped, there are many questions unanswered. We are interested in using mass spectrometry to evaluate the distribution and localization of the compound in the CNS, specifically the brain as a way of preclinical evaluations of future nitroimidazole candidates.

1.1.3. Mass spectrometry

Mass spectrometry (MS) remains a prominent, sensitive and accurate analytical tool that can give a full chemical composition of a sample and it only requires a small sample [55, 56]. An MS instrument consists of three key parts; an ionization source, a mass analyzer and a detector. During the MS analysis, the sample is first introduced into the ionization source which converts them into ions in the form of gas. The ions move through the mass analyzer which separates them per their mass-to-charge ratios (*m/z*). The separation process occurs under vacuum which helps to prevent collision of target ions with other unwanted molecules. Inside the mass analyzer, there are focusing lenses which are used to direct the ions towards the detector

and it generates electrical signals that are proportional to the number of ions formed. The electrical signals are then recorded by the computer for further analysis.

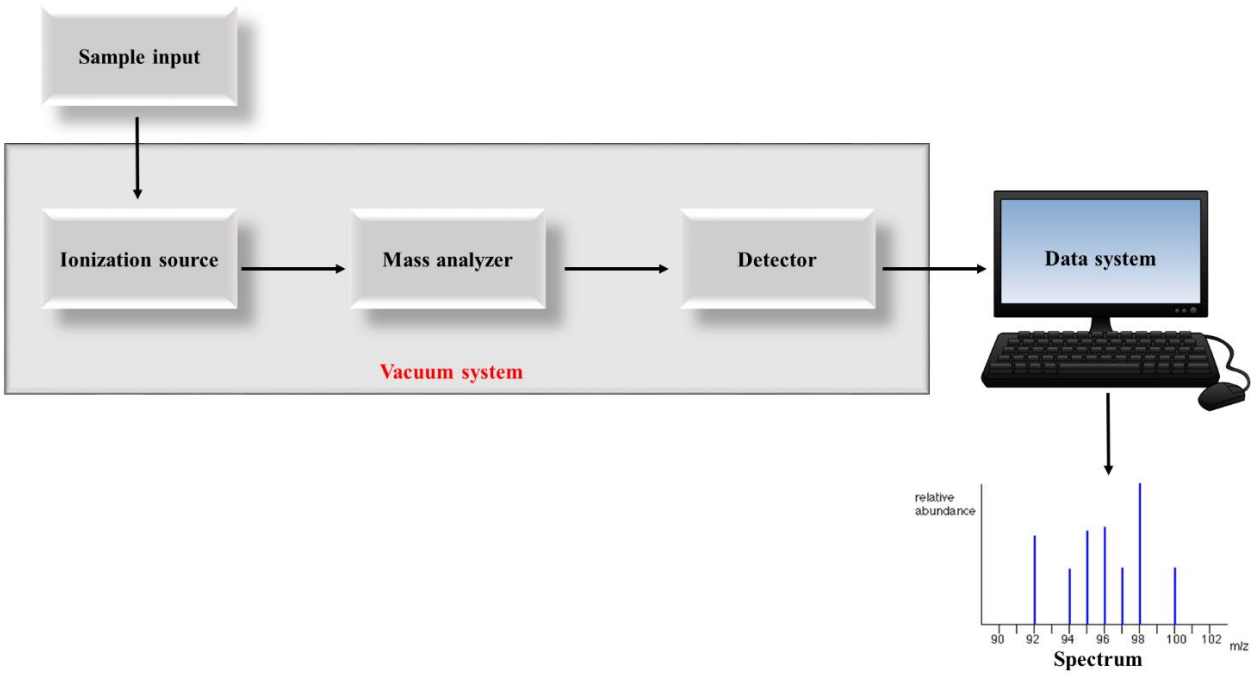

Figure 1.3. Different components of a mass spectrometer (some parts of this diagram were obtained from Computer clipart [57] and Chemguide [58] websites).

The choice of the ionization source relies on the specific nature of the sample. Often, MS is coupled to chromatographic systems such as liquid chromatography (LC) and gas chromatography (GC). The sample from the LC is in the liquid phase, but for mass spectrometry, the sample must be in an ionized gas form. There are different ionization techniques that are applied to convert the sample into an ionized gas form. There are soft and hard ionization techniques. Electron ionization (EI) [59, 60] is a hard ionization method and is one of the first techniques for MS. Several soft ionization methods include, matrix-assisted laser desorption/ionization (MALDI) [61, 62] atmospheric pressure chemical ionization (APCI) [63, 64], fast atom bombardment (FAB) [65, 66], electrospray ionization (ESI) [55, 67] and chemical ionization (CI) [68].

Several modern mass analyzers used in drug development include time-of-flight (TOF) [69, 70], quadrupole [71], Fourier transform ion cyclotron resonance (FT-ICR) [72, 73], magnetic sector [74], ion trap [75] and hybrid mass analyzers. From all of the mentioned mass analyzers, TOF is regarded as one of the most uncomplicated mass analyzers [76]. TOF uses constant voltages to accelerate the ions through to the detector [77]. The velocity of each charged ion as it travels through the flight tube (under vacuum) depends

on its *m/z*. Thus, light-weight ions have a much faster movement through the TOF tube compared to heavier ions and that results in good resolution, high mass accuracy and selectivity. The TOF mass analyzers allow the determination of *m/z* for smaller and larger molecules and they have high sensitivity, accuracy and wide mass range [78].

LC-MS/MS methods have proven to be productive in drug development, toxicology, pre-clinical and clinical studies [79-81]. Hyphenating the MS to chromatographic systems has remained preferable because of high sensitivity, incredible detection limits, a wide range of applications and highly distinct characteristics of MS in comparison to other chromatographic detectors [68]. The reliability of analytical data is of high priority in the biomedical research field for the correct interpretation of findings. Quantitative analytical methods used in biological samples are the important determining factors in producing true and reliable data to evaluate and interpret the bioavailability, toxicokinetic, pharmacokinetic and bioequivalence results [82]. Full bioanalytical method validation is essential, especially for new drugs to be analyzed for the first time. The results obtained are further used to make very critical conclusions based the safety and efficacy of such drugs [83]. Previously, we have investigated the pharmacokinetics and tissue distribution of different antibiotics using LC-MS/MS methods [84-86]. In this study, an LC-MS/MS method was validated based on bioanalytical guidelines set by the European Medicines Agency (EMA) and then applied to a pharmacokinetic and tissue distribution study of TBA-354. As advanced as LC-MS/MS methods are, they have some limitations, i.e. they cannot provide information about the specific location of the target compound in different regions of a studied organ (brain, lung, kidney etc.). That kind of information can be gathered using imaging techniques such as MALDI-MSI.

1.1.4. MALDI-MSI

MALDI-MSI is one of the emerging techniques that favors mapping of a broad range of compounds (large non-volatile biomolecules for instance peptides, proteins and smaller molecules like drugs and their metabolites) directly from tissue samples [87]. MALDI-MSI has been widely employed in the biomedical research field [88], where it is used to investigate and monitor drug distribution and metabolism in various organs (e.g. liver, kidney, lung, brain and etc.). MALDI-MSI has been evolving since the first imaging experiment in 1997 [89]. In terms of technological improvements, several sample preparation protocols have been established to simplifying the study of different compounds with improved high-resolution images [90, 91]. Unlike other imaging techniques, for instance, magnetic resonance imaging (MRI) and positron emission tomography (PET), MALDI-MSI cannot be used to map compounds in a living body, but it still has a significant role in preclinical studies [92]. The one advantage that makes MSI superior to other imaging techniques is that a wide range of compounds spatially distributed on a biological tissue sample can be mapped without any prior nuclear labeling [93]. Enough data can be obtained without going

through several complex sample preparation steps. There is still an ongoing research on improvements of MALDI-MSI experiments concerning the enhancement of the image resolution [94, 95], sample preparation optimization [96] and the sensitivity of the instruments [97].

The general principles of MALDI-MSI depend on the direct analysis of biological tissue samples. Sample preparation is a very crucial step in MSI methods. The first step involves the uniform application of the MALDI matrices onto the tissue sample. There are two main roles of the MALDI matrix: to help extract analyte molecules from the tissues sample and to facilitate the desorption-ionization process which results in the formation of ions that are further analyzed by the mass analyzer [98, 99]. Usually, aromatic organic compounds are used as matrix since they strongly absorbed ultraviolet (UV) laser energy. The selection of a suitable matrix is a crucial step in MSI methods because it plays an important role to ionize the analyte, which is reflected in the quality of the spectra produced. Usually, the tissue slices are thaw-mounted onto conductive microscope slides and a compatible matrix must be applied uniformly onto the tissue sample. Spray-coating is one technique that is normally employed in MSI to achieve uniform application of the matrix onto the tissue sample [99, 100]. The matrix is sprayed as an aerosol onto the tissue sample and then allowed to dry under inert conditions (nitrogen gas normally used) [101]. The spray-coating technique involves different phases where the process is repeated for several times until there is enough matrix on the surface. Other techniques include matrix sublimation and micro spotting [102]. In sublimation, the matrix is heated and converted into vapor then allowed to condense onto the sample and the thickness and the size of the crystal can be controlled by adjusting the heat applied to the matrix [103].

UV laser beam is used as the source of ionization energy. Thus, the matrix must be UV active to facilitate ionization process. Once the slides are prepared, they are placed into the ionization chamber and the sample is then irradiated by a pulsed powerful ultraviolet laser beam [100, 104]. The energy of the laser is absorbed by the matrix and transferred to the analyte molecules, resulting in rapid desorption and ionization of both the analyte and matrix from the target spot. Finally, the ions formed are accelerated and directed to the mass analyzer where they are analyzed per their *m/z* values. When ions reach the detector, they are immediately converted to *m/z* signals. The data appears as a plot of intensity *vs m/z*.

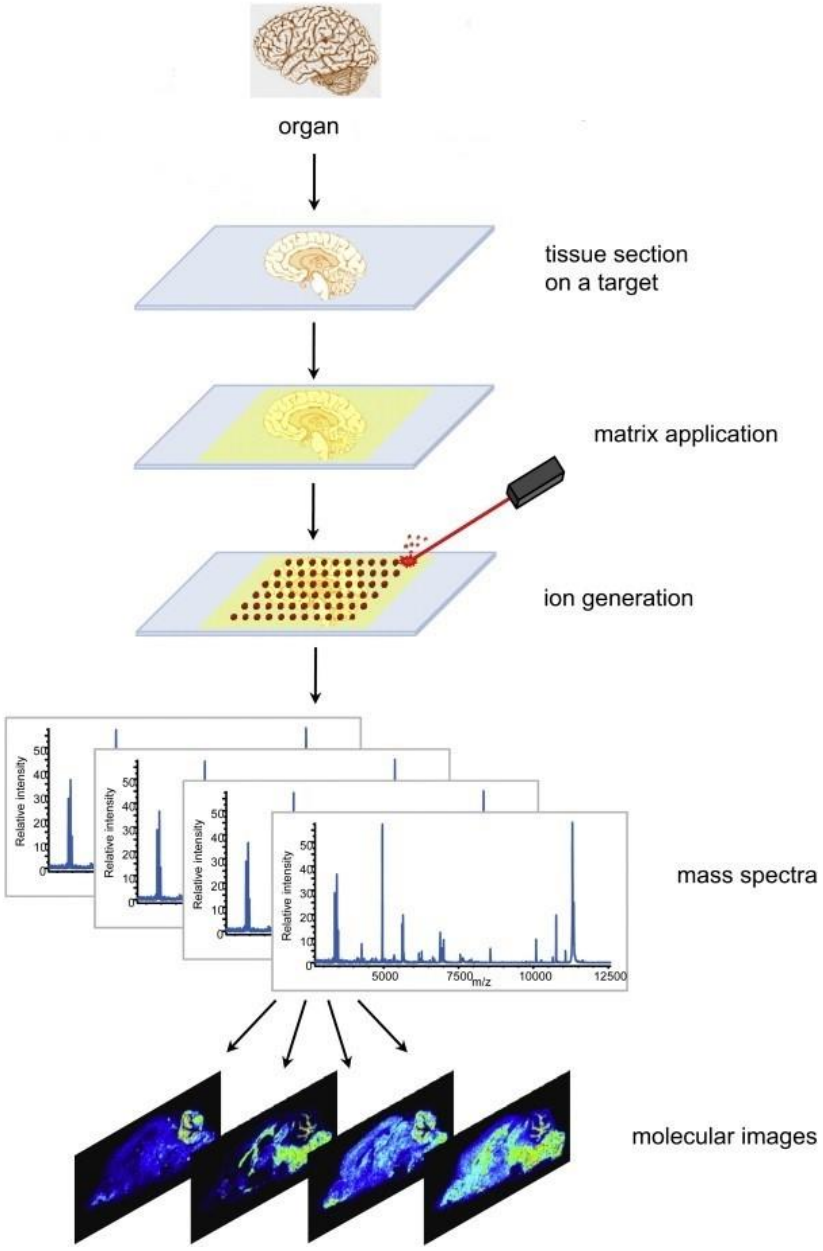

Figure 1.4. The standard workflow of MALDI-MSI experiments [105].

A lot of work has been done on investigating the drug distribution of anti-TB drugs and other antibiotics in tissue samples using MALDI-MSI [102, 106, 107]. Previously we have conducted studies based on the evaluation of the molecular histology of various anti-TB drugs such as linezolid [86], rifampicin [93], clofazimine [32], pretomanid [33] and fluoroquinolones [31]. In this study, we used the MALDI-MSI technique to examine the distribution and localization of TBA-354 in the rat brain.

1.2. Aims and objectives of the study

Aim 1: To evaluate the fundamental pharmacokinetic and tissue distribution properties of TBA-354 in a rat model using LC-MS/MS.

a) Objective 1: To develop and validate a simple, sensitive and reproducible LC-MS/MS method for the quantification of TBA-354 in rat plasma, lung and brain homogenates.

b) Objective 2: To assess the pharmacokinetics and tissue distribution (C_{max}, T_{max} and $t_{1/2}$, AUC) of intraperitoneally administered TBA-345 in rat plasma, lung and brain.

c) Objective 3: Compare the concentration levels and pharmacokinetic parameters of TBA-354 in rat plasma, lung and brain homogenate samples.

Aim 2: To evaluate the neurotoxic potential of TBA-354 using the MALDI-MSI technique.

a) Objective 1: To investigate the distribution and localization of TBA-354 in the rat brain *via* the MALDI-MSI technique.

b) Objective 2: To investigate the brain regional variations of TBA-354 per time interval.

1.3. Outline of this thesis

This study involved the development of mass spectrometric methods which can be used in pre-clinical investigations of a new anti-TB nitroimidazole derivative, TBA-354. The following chapter (Chapter 2**)** presents the research results (The downfall of TBA-354 – investigating its neurotoxicity in the brain using mass spectrometry). Chapter 3 consists of the general discussion and conclusions of the study.

1.4. References

1. Lamrabet, O. and M. Drancourt, *Genetic engineering of Mycobacterium tuberculosis: A review.* Tuberculosis, 2012. **92**: p. 365-376.
2. World Health Organization. *Global tuberculosis report*, 2016. [cited 2016 21 October]; Available from: http://apps.who.int/iris/bitstream/10665/250441/1/9789241565394-eng.pdf?ua=1.
3. Sileshi, B., et al., *Predictors of mortality among TB-HIV Co-infected patients being treated for tuberculosis in Northwest Ethiopia: a retrospective cohort study.* BMC Infectious Diseases, 2013. **13**: p. 297-297.
4. Naidoo, P., et al., *Predictors of knowledge about tuberculosis: results from SANHANES I, a national, cross-sectional household survey in South Africa.* BMC public health, 2016. **16**: p. 1-13.
5. Sharma, S., A. Mohan, and T. Kadhiravan, *HIV-TB co-infection: epidemiology, diagnosis & management.* Indian Journal of Medical Research, 2005. **121**: p. 550-562.
6. Kwan, C.K. and J.D. Ernst, *HIV and Tuberculosis: a Deadly Human Syndemic.* Clinical Microbiology Reviews, 2011. **24**: p. 351-376.
7. Padmapriyadarsini, C., G. Narendran, and S. Swaminathan, *Diagnosis & treatment of tuberculosis in HIV co-infected patients.* The Indian Journal of Medical Research, 2011. **134**: p. 850-865.
8. Burman, W.J., *Issues in the Management of HIV-Related Tuberculosis.* Clinics in Chest Medicine, 2005. **26**: p. 283-294.
9. Daniel, T.M., *The history of tuberculosis.* Respiratory Medicine, 2006. **100**: p. 1862-1870.
10. Comroe, J.H., *Pay Dirt: The Story of Streptomycin.* American Review of Respiratory Disease, 1978. **117**: p. 773-781.
11. Lehmann, J., *PARA-AMINOSALICYLIC ACID IN THE TREATMENT OF TUBERCULOSIS.* The Lancet, 1946. **247**: p. 15-16.
12. Tiemersma, E.W., et al., *Natural History of Tuberculosis: Duration and Fatality of Untreated Pulmonary Tuberculosis in HIV Negative Patients: A Systematic Review.* PLoS ONE, 2011. **6**: p. e17601.
13. World Health Organization. *Global tuberculosis report*, 2015. [cited 2016 21 October]; Available from: http://apps.who.int/iris/bitstream/10665/191102/1/9789241565059_eng.pdf.

14. Fu, L.M. and S.C. Tai, *The Differential Gene Expression Pattern of Mycobacterium tuberculosis in Response to Capreomycin and PA-824 versus First-Line TB Drugs Reveals Stress- and PE/PPE-Related Drug Targets.* International Journal of Microbiology, 2009. **2009**: p. 9-27.

15. Espinal, M.A., *The global situation of MDR-TB.* Tuberculosis, 2003. **83**: p. 44-51.

16. Farmer, P., et al., *The dilemma of MDR-TB in the global era [Counterpoint]*. The International Journal of Tuberculosis and Lung Disease, 1998. **2**: p. 869-876.

17. Migliori, G., et al., *125 years after Robert Koch's discovery of the tubercle bacillus: the new XDR-TB threat. Is "science" enough to tackle the epidemic?* European Respiratory Journal, 2007. **29**: p. 423-427.

18. Mugunthan, G., et al., *Synthesis and screening of galactose-linked nitroimidazoles and triazoles against Mycobacterium tuberculosis.* European Journal of Medicinal Chemistry, 2011. **46**: p. 4725-4732.

19. Duncan, K. and C.E. Barry Iii, *Prospects for new antitubercular drugs.* Current Opinion in Microbiology, 2004. **7**: p. 460-465.

20. López-Gavín, A., et al., *In vitro activity against Mycobacterium tuberculosis of levofloxacin, moxifloxacin and UB-8902 in combination with clofazimine and pretomanid.* International Journal of Antimicrobial Agents, 2015. **46**: p. 582-585.

21. Pala, K., et al., *30 Years Retrospective Review of Tuberculosis Cases in a Tuberculosis Dispensary in Bursa/Nilufer, Turkey (1985-2014).* Mediterranean Journal of Hematology and Infectious Diseases, 2016. **8**: p. 32-59.

22. Norbis, L., et al., *Challenges and perspectives in the diagnosis of extrapulmonary tuberculosis.* Expert Review of Anti-infective Therapy, 2014. **12**: p. 633-647.

23. Marouane, C., et al., *Evaluation of molecular detection of extrapulmonary tuberculosis and resistance to rifampicin with GeneXpert® MTB/RIF*. Médecine et Maladies Infectieuses, 2016. **46**: p. 20-24.

24. Raveendran, R. and C. Wattal, *Utility of multiplex real-time PCR in the diagnosis of extrapulmonary tuberculosis.* The Brazilian Journal of Infectious Diseases, 2016. **20**: p. 235-241.

25. Frieden, T.R., et al., *Tuberculosis.* The Lancet, 2003. **362**(9387): p. 887-899.

26. Török, M.E., *Tuberculous meningitis: advances in diagnosis and treatment.* British Medical Bulletin, 2015. **113**: p. 117-131.

27. *Tuberculous Meningitis: Diagnosis and Treatment Overview.* Tuberculosis Research and Treatment, 2011. **2011**: p. 1-9

28. Mai, N.T.H. and G.E. Thwaites, *The current pharmacological landscape of tuberculous meningitis: where to next?* Expert Review of Clinical Pharmacology, 2016. **9**: p. 625-627.

29. Kalita, J., et al., *Safety and efficacy of levofloxacin versus rifampicin in tuberculous meningitis: an open-label randomized controlled trial.* Journal of Antimicrobial Chemotherapy, 2014. **69**: p. 2246-2251.

30. TB-Alliance. *Clinical Development and Marketed Products*, 2016. [cited 2016 23 November]; Available from: https://www.tballiance.org/portfolio/.

31. Shobo, A., et al., *MALDI MSI and LC-MS/MS: Towards preclinical determination of the neurotoxic potential of fluoroquinolones.* Drug Testing and Analysis, 2016. **8**: p. 832-838.

32. Baijnath, S., et al., *Evidence for the presence of clofazimine and its distribution in the healthy mouse brain.* Journal of Molecular Histology, 2015. **46**: p. 439-442.

33. Shobo, A., et al., *Tissue distribution of pretomanid in rat brain via mass spectrometry imaging.* Xenobiotica, 2016. **46**: p. 247-252.

34. Cudmore, S.L., et al., *Treatment of Infections Caused by Metronidazole-Resistant Trichomonas vaginalis.* Clinical Microbiology Reviews, 2004. **17**: p. 783-793.

35. Pearlman, M.D., et al., *An incremental dosing protocol for women with severe vaginal trichomoniasis and adverse reactions to metronidazole.* American Journal of Obstetrics and Gynecology, 1996. **174**: p. 934-936.

36. Voogd, C.E., *On the mutagenicity of nitroimidazoles.* Mutation Research/Reviews in Genetic Toxicology, 1981. **86**: p. 243-277.

37. Upcroft, J.A., et al., *5-Nitroimidazole Drugs Effective against Metronidazole-Resistant Trichomonas vaginalis and Giardia duodenalis.* Antimicrobial Agents and Chemotherapy, 2006. **50**: p. 344-347.

38. Veldhuyzen van Zanten, S.J., P.M. Sherman, and R.H. Hunt, *Helicobacter pylori: new developments and treatments.* CMAJ: Canadian Medical Association Journal, 1997. **156**: p. 1565-1574.

39. Mukherjee, T. and H. Boshoff, *Nitroimidazoles for the treatment of TB: past, present and future.* Future medicinal chemistry, 2011. **3**: p. 1427-1454.

40. Upton, A.M., et al., *In Vitro and In Vivo Activities of the Nitroimidazole TBA-354 against Mycobacterium tuberculosis.* Antimicrobial Agents and Chemotherapy, 2015. **59**: p. 136-144.

41. Khan, A., S. Sarkar, and D. Sarkar, *Bactericidal activity of 2-nitroimidazole against the active replicating stage of Mycobacterium bovis BCG and Mycobacterium tuberculosis with intracellular efficacy in THP-1 macrophages.* International Journal of Antimicrobial Agents, 2008. **32**: p. 40-45.

42. Jallapally, A., et al., *2-Butyl-4-chloroimidazole based substituted piperazine-thiosemicarbazone hybrids as potent inhibitors of Mycobacterium tuberculosis.* Bioorganic & Medicinal Chemistry Letters, 2014. **24**: p. 5520-5524.

43. [No authors listed]. *OPC-67683.* Tuberculosis, 2008. **88**: p. 132-133.

44. Rakesh, et al., *Synthesis and evaluation of pretomanid (PA-824) oxazolidinone hybrids.* Bioorganic & Medicinal Chemistry Letters, 2016. **26**: p. 388-391.

45. Ashtekar, D.R., et al., *In vitro and in vivo activities of the nitroimidazole CGI 17341 against Mycobacterium tuberculosis.* Antimicrobial Agents and Chemotherapy, 1993. **37**: p. 183-186.

46. TB-Alliance. *PA-824 has a New Generic Name: Pretomanid*, 2014. [cited 2016 21 November]; Available from: https://www.tballiance.org/news/pa-824-has-new-generic-name-pretomanid.

47. TB-Alliance. *Phase 1 Clinical Trial of TB Drug Candidate TBA-354 Discontinued*, 2016. [cited 2016 20 May]; Available from: http://www.tballiance.org/news/phase-1-clinical-trial-tb-drug-candidate-tba-354-discontinued.

48. Haver, H.L., et al., *Mutations in Genes for the F420 Biosynthetic Pathway and a Nitroreductase Enzyme Are the Primary Resistance Determinants in Spontaneous In Vitro-Selected PA-824-Resistant Mutants of Mycobacterium tuberculosis.* Antimicrobial Agents and Chemotherapy, 2015. **59**: p. 5316-5323.

49. Manjunatha, U.H., et al., *Identification of a nitroimidazo-oxazine-specific protein involved in PA-824 resistance in Mycobacterium tuberculosis.* Proceedings of the National Academy of Sciences of the United States of America, 2006. **103**: p. 431-436.

50. Manjunatha, U., H.I.M. Boshoff, and C.E. Barry, *The mechanism of action of PA-824: Novel insights from transcriptional profiling.* Communicative & Integrative Biology, 2009. **2**: p. 215-218.

51. Gupta, R., et al., *Delamanid for Extensively Drug-Resistant Tuberculosis.* New England Journal of Medicine, 2015. **373**: p. 291-292.

52. Ryan, N.J. and J.H. Lo, *Delamanid: First Global Approval.* Drugs, 2014. **74**: p. 1041-1045.

53. Tasneen, R., et al., *Contribution of the Nitroimidazoles PA-824 and TBA-354 to the Activity of Novel Regimens in Murine Models of Tuberculosis.* Antimicrobial Agents and Chemotherapy, 2015. **59**: p. 129-135.

54. i-Base. *The tuberculosis treatment pipeline: activity, but no answers*, 2016. [cited 2016 04 October]; Available from: http://i-base.info/htb/30164

55. Ho, C.S., et al., *Electrospray Ionisation Mass Spectrometry: Principles and Clinical Applications.* The Clinical Biochemist Reviews, 2003. **24**: p. 3-12.

56. Perez-Lao, E., J.E. Sanchez-Galan, and R.A. Gittens. *Assessing the performance of different sample targets for a MALDI-TOF mass spectrometer*. in *Central America and Panama Convention (CONCAPAN XXXIV), 2014 IEEE*. 2014.

57. Clipartion. *Computer Clipart*. 2015 [cited 2016 24 November]; Available from: https://clipartion.com/free-clipart-computer-clipart/.

58. Clark, J. *THE MASS SPECTROMETER*, 2015. [cited 2016 24 November]; Available from: http://www.chemguide.co.uk/analysis/masspec/howitworks.html.

59. Kieffer, L.J. and G.H. Dunn, *Electron Impact Ionization Cross-Section Data for Atoms, Atomic Ions, and Diatomic Molecules: I. Experimental Data.* Reviews of Modern Physics, 1966. **38**: p. 1-35.

60. Märk, T.D. and G.H. Dunn, *Electron Impact Ionization* . Springer Vienna. 2013: p. 24-41.

61. Karas, M. and R. Krüger, *Ion Formation in MALDI: The Cluster Ionization Mechanism.* Chemical Reviews, 2003. **103**: p. 427-440.

62. Knochenmuss, R., *Ion formation mechanisms in UV-MALDI.* Analyst, 2006. **131**: p. 966-986.

63. Carroll, D.I., et al., *Subpicogram detection system for gas phase analysis based upon atmospheric pressure ionization (API) mass spectrometry.* Analytical Chemistry, 1974. **46**: p. 706-710.

64. Marchi, I., S. Rudaz, and J.-L. Veuthey, *Atmospheric pressure photoionization for coupling liquid-chromatography to mass spectrometry: A review*. Talanta, 2009. **78**: p. 1-18.

65. Morris, H.R., et al., *Fast atom bombardment: A new mass spectrometric method for peptide sequence analysis.* Biochemical and Biophysical Research Communications, 1981. **101**: p. 623-631.

66. Barber, M., et al., *Fast Atom Bombardment Mass Spectrometry.* Analytical Chemistry, 1982. **54**: p. 645A-657A.

67. Loo, J.A., *Electrospray ionization mass spectrometry: a technology for studying noncovalent macromolecular complexes.* International Journal of Mass Spectrometry, 2000. **200**: p. 175-186.

68. Pitt, J.J., *Principles and Applications of Liquid Chromatography-Mass Spectrometry in Clinical Biochemistry*. The Clinical Biochemist Reviews, 2009. **30**: p. 19-34.

69. Campana, J.E., *Time-of-Flight Mass Spectrometry: a Historical Overview*. Instrumentation Science & Technology, 1987. **16**: p. 1-14.

70. Mirsaleh-Kohan, N., W.D. Robertson, and R.N. Compton, *Electron ionization time-of-flight mass spectrometry: Historical review and current applications.* Mass Spectrometry Reviews, 2008. **27**: p. 237-285.

71. Yost, R.A. and C.G. Enke, *Triple Quadrupole Mass Spectrometry*. Analytical Chemistry, 1979. **51**: p. 1251A-1264A.

72. Marshall, A.G., C.L. Hendrickson, and G.S. Jackson, *Fourier transform ion cyclotron resonance mass spectrometry: a primer*. Mass spectrometry reviews, 1998. **17**: p. 1-35.

73. Marshall, A.G., *Fourier transform ion cyclotron resonance mass spectrometry*. Accounts of Chemical Research, 1985. **18**: p. 316-322.

74. Bateman, R.H. and P. Burns, *Magnetic sector mass spectrometer*, 1988, Google Patents.

75. Cooks, R.G., et al., *Ion Trap Mass Spectrometry.* Chemical & Engineering News Archive, 1991. **69**: p. 26-41.

76. Wang, P.G., M.F. Vitha, and J.F. Kay, *High Throughput Analysis for Food Safety*. 2014: Wiley.

77. Williamson, L.N. and M.G. Bartlett, *Quantitative liquid chromatography/time-of-flight mass spectrometry*. Biomedical Chromatography, 2007. **21**: p. 567-576.

78. Bristow, A.W.T., *Accurate mass measurement for the determination of elemental formula—A tutorial.* Mass Spectrometry Reviews, 2006. **25**: p. 99-111.

79. Jenkins, K.M., et al., *Automated high throughput ADME assays for metabolic stability and cytochrome P450 inhibition profiling of combinatorial libraries.* Journal of Pharmaceutical and Biomedical Analysis, 2004. **34**: p. 989-1004.

80. Korfmacher, W.A., *Foundation review: Principles and applications of LC-MS in new drug discovery*. Drug Discovery Today, 2005. **10**: p. 1357-1367.

81. Wang, L., et al., *Pharmacokinetics and tissue distribution study of PA-824 in rats by LC–MS/MS.* Journal of Chromatography B, 2015. **1006**: p. 194-200.

82. Shah, V.P., et al., *Bioanalytical Method Validation—A Revisit with a Decade of Progress.* Pharmaceutical Research, 2000. **17**: p. 1551-1557.

83. E.M.A. *European Medicines Agency, C.H.M.P. Committee for Medicinal Products for Human Use*, 2009. [cited 2016 15 March]; Available from: http://www.ema.europa.eu/docs/en_GB/document_library/Scientific_guideline/2011/08/WC500109686.pdf.

84. Bratkowska, D., et al., *Determination of the antitubercular drug PA-824 in rat plasma, lung and brain tissues by liquid chromatography tandem mass spectrometry: Application to a pharmacokinetic study.* Journal of Chromatography B, 2015. **988**: p. 187-194.

85. Munyeza, C.F., et al., *Rapid and widespread distribution of doxycycline in rat brain: a mass spectrometric imaging study.* Xenobiotica, 2016. **46**: p. 385-392.

86. Baijnath, S., et al., *Neuroprotective potential of Linezolid: a quantitative and distribution study via mass spectrometry.* Journal of Molecular Histology, 2016. **47**: p. 429-435.

87. McDonnell, L.A. and R.M.A. Heeren, *Imaging mass spectrometry.* Mass Spectrometry Reviews, 2007. **26**: p. 606-643.

88. Aichler, M. and A. Walch, *MALDI Imaging mass spectrometry: current frontiers and perspectives in pathology research and practice.* Laboratory Investigation, 2015. **95**: p. 422-431.

89. Caprioli, R.M., T.B. Farmer, and J. Gile, *Molecular Imaging of Biological Samples: Localization of Peptides and Proteins Using MALDI-TOF MS.* Analytical Chemistry, 1997. **69**: p. 4751-4760.

90. Schubert, S., et al., *Novel, Improved Sample Preparation for Rapid, Direct Identification from Positive Blood Cultures Using Matrix-Assisted Laser Desorption/Ionization Time-of-Flight (MALDI-TOF) Mass Spectrometry.* The Journal of Molecular Diagnostics, 2011. **13**: p. 701-706.

91. Nordhoff, E., et al., *Sample preparation protocols for MALDI-MS of peptides and oligonucleotides using prestructured sample supports.* International Journal of Mass Spectrometry, 2003. **226**: p. 163-180.

92. Zhang, Y., et al., *Combination of ESI and MALDI mass spectrometry for qualitative, semi-quantitative and in situ analysis of gangliosides in brain.* Scientific Reports, 2016. **6**: p. 25289-25300.

93. Shobo, A., et al., *Visualization of Time-Dependent Distribution of Rifampicin in Rat Brain Using MALDI MSI and Quantitative LCMS/MS.* ASSAY and Drug Development Technologies, 2015. **13**: p. 277-284.

94. Martin-Lorenzo, M., et al., *30 μm spatial resolution protein MALDI MSI: In-depth comparison of five sample preparation protocols applied to human healthy and atherosclerotic arteries.* Journal of Proteomics, 2014. **108**: p. 465-468.

95. Leinweber, B.D., et al., *Improved MALDI-TOF Imaging Yields Increased Protein Signals at High Molecular Mass.* Journal of the American Society for Mass Spectrometry, 2009. **20**: p. 89-95.

96. Tisdale, E., D. Kennedy, and C. Wilkins, *Matrix-assisted laser desorption/ionization sample preparation optimization for structural characterization of poly(styrene-co-pentafluorostyrene) copolymers.* Analytica Chimica Acta, 2014. **808**: p. 151-162.

97. Peng, L. and G.R. Kinsel, *Improving the sensitivity of matrix-assisted laser desorption/ionization (MALDI) mass spectrometry by using polyethylene glycol modified polyurethane MALDI target.* Analytical Biochemistry, 2010. **400**: p. 56-60.

98. Jaskolla, T.W., W.-D. Lehmann, and M. Karas, *4-Chloro-α-cyanocinnamic acid is an advanced, rationally designed MALDI matrix.* Proceedings of the National Academy of Sciences, 2008. **105**: p. 12200-12205.

99. Amstalden van Hove, E.R., D.F. Smith, and R.M.A. Heeren, *A concise review of mass spectrometry imaging.* Journal of Chromatography A, 2010. **1217**: p. 3946-3954.

100. Zenobi, R. and R. Knochenmuss, *Ion formation in MALDI mass spectrometry.* Mass Spectrometry Reviews, 1998. **17**: p. 337-366.

101. Norris, J.L. and R.M. Caprioli, *Analysis of Tissue Specimens by Matrix-Assisted Laser Desorption/Ionization Imaging Mass Spectrometry in Biological and Clinical Research.* Chemical Reviews, 2013. **113**: p. 2309-2342.

102. Castellino, S., M.R. Groseclose, and D. Wagner, *MALDI imaging mass spectrometry: bridging biology and chemistry in drug development.* Bioanalysis, 2011. **3**: p. 2427-2441.

103. Hankin, J.A., R.M. Barkley, and R.C. Murphy, *Sublimation as a method of matrix application for mass spectrometric imaging.* Journal of the American Society for Mass Spectrometry, 2007. **18**: p. 1646-1652.

104. Marvin, L.F., M.A. Roberts, and L.B. Fay, *Matrix-assisted laser desorption/ionization time-of-flight mass spectrometry in clinical chemistry.* Clinica Chimica Acta, 2003. **337**: p. 11-21.

105. Schwamborn, K. and R.M. Caprioli, *MALDI Imaging Mass Spectrometry – Painting Molecular Pictures.* Molecular Oncology, 2010. **4**: p. 529-538.

106. Trim, P.J. and M.F. Snel, *Small molecule MALDI MS imaging: Current technologies and future challenges.* Methods, 2016. **104**: p. 127-141.

107. Prideaux, B., et al., *High-Sensitivity MALDI-MRM-MS Imaging of Moxifloxacin Distribution in Tuberculosis-Infected Rabbit Lungs and Granulomatous Lesions.* Analytical Chemistry, 2011. **83**: p. 2112-2118.

Chapter 2

The downfall of TBA-354 – investigating its neurotoxicity in the brain using mass spectrometry

The downfall of TBA-354 – investigating its neurotoxicity in the brain using mass spectrometry

Sphamandla Ntshangase[1], Sooraj Baijnath[1], Adeola Shobo[1], Sanil D. Singh[2], Glenn Maguire[1], Gert Kruger[1], Per Arvidsson[1,3], Tricia Naicker[1], Thavendran Govender[1]

[1] Catalysis and Peptide Research Unit, University of KwaZulu-Natal, Westville Campus, Durban, South Africa.

[2] Biomedical Resource Unit, University of KwaZulu-Natal, Westville Campus, Durban, South Africa.

[3]Science for Life Laboratory, Drug Discovery & Development Platform & Division of Translational Medicine and Chemical Biology, Development of Medical Biochemistry and Biophysics, Karolinska Institutet, Stockholm, Sweden

Corresponding author:

Professor Thavendran Govender

Catalysis and Peptide Research Unit

E-block, 6th floor, Room E1-06-016

University of KwaZulu-Natal, Westville Campus, South Africa

Offices: +27 31 260 8212/1845/1799

Cell: +27732625616

Email address: govenderthav@ukzn.ac.za

1.1. Highlights

- We hereby prove the use of mass spectrometric imaging (MSI) as a preclinical tool for evaluating the potential of nitroimidazole antibiotics
- MSI investigations showed that TBA-354 distributes and accumulates in the neocortex brain region thereby offering an explanation for the neurological toxicity that led to the end of clinical trials for this compound
- This paper is the first to present a validated method for the quantification of TBA-354 in rat plasma, lung and brain homogenates

Keywords: Mass spectrometric imaging; TBA-354; pharmacokinetics; nitroimidazoles; plasma; lung homogenate; brain homogenate

2.2. Abstract

Background: TBA-354 is a bicyclic nitroimidazole derivative that has potent antitubercular activity against both replicating and static *Mycobacterium tuberculosis* (*M.tb*) bacteria strains. There have been concerns about TBA-354 having mild signs of neurotoxicity which left the TB alliance with no other choice but to discontinue the clinical trials.

Objectives: In this study, we aimed to develop mass spectrometric methods to understand the preclinical pharmacokinetics and spatial distribution of the compound via a validated quantitative liquid chromatography-tandem mass spectrometry (LC-MS/MS) method and matrix-assisted laser desorption/ionization-mass spectrometric imaging (MALDI-MSI).

Methods: Three healthy female Sprague-Dawley rats per group received intraperitoneal (i.p.) injections of TBA-354 at a dose of 20 mg/kg. Biological samples (plasma, lung and brain) were collected at 0, 0.25, 0.5, 1, 2, 4, 6, 8 and 24 h postdose. TBA-354 was quantified from the three biological samples using LC-MS/MS to determine its pharmacokinetic tissue distribution. Spatial distribution of TBA-354 in brain tissues was done via MALDI-MSI.

Results: The concentration-time profiles showed a gradual absorption and distribution of TBA-354 reaching the C_{max} at 6.00 h postdose followed by the rapid elimination in all three biological samples. MSI analysis provided detailed time-dependent drug distribution, with an accumulation observed in the neocortical regions of the brain.

Conclusion: This study provides the evidence as to why TBA-354 showed certain neurotoxic signs during the clinical trials. These results demonstrate the importance that MSI can play role in preclinical evaluations for this class of compounds for drug discovery.

2.3. Introduction

There were 10.4 million recorded tuberculosis (TB) cases across the world in 2015 and TB continues to be a significant global health concern [1]. *Mycobacterium tuberculosis* (*M.tb*), the causative bacteria, has developed resistance to some anti-TB drugs and evolved into strains which are either extremely drug resistant (XDR-TB) or multi-drug resistant (MDR-TB). These forms of TB are not susceptible to any of the fluoroquinolones and to the second-line anti-TB drugs such as kanamycin, capreomycin, and amikacin [2]. The major issues in drug development, are that anti-TB drug candidates are either less effective, have unacceptable side effects or expensive to produce and purchase. This highlights the need for the development of effective compounds, focusing on improvements in therapy times and fighting the current global problem of rapidly emerging MDR-TB and XDR-TB. These resistant TB strains are thought to be the cause of the prolonged chemotherapy required to cure patients [3]. Several novel anti-tubercular drug classes have shown promise in shortening chemotherapy in pre-clinical studies [4-7].

Nitroimidazoles, are an encouraging class of antitubercular agents that has caught researcher's interest in the last decades. Drug development for TB has been focused on the use of nitroimidazole drugs due to their novel mechanism of action and lower probability of developing resistance to different *M.tb* strains [8]. The 2-nitroimidazoles were the first drugs of this class to exhibit activity against *M.tb* [9]. The bicyclic nitroimidazole derivative, pretomanid, also known as PA-824 was not mutagenic and showed potent activity against both multiplying and non-replicating *M.tb*, including MDR-TB [4, 10]. Pretomanid is currently in Phase 3 clinical trials where it is in a promising combinatory study with moxifloxacin and pyrazinamide. Delamanid is another bicyclic nitroimidazole that has recently been approved by the European Union to be used in the treatment of MDR-TB [11].

TBA-354 (**Figure 2.1**) is nitroimidazole derivative that has a more potent anti-TB activity than pretomanid with a similar mode of action (**Figure 2.1**) and is the latest member of this promising class of drugs [12, 13]. A recent report stated that TBA-354 is more active than pretomanid, both *in-vitro* and *in-vivo* [14]. The *in-vivo* results have confirmed that TBA-354 has a higher bioavailability and longer half-life when compared to other nitroimidazole derivatives which are presently in clinical trials. The *in-vitro* studies showed that this anti-tubercular compound has a minimum inhibitory concentration (MIC) less than 0.36 µM (156.96 ng/mL) against ten different *M.tb* strains which makes it the focal point of pre-clinical and clinical trials [14].

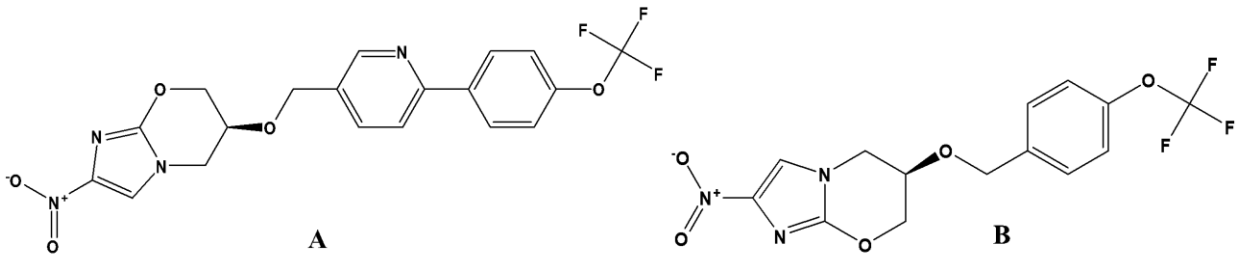

Figure 2.1. Chemical structures of TBA-354 (A: target analyte) and pretomanid (B: internal standard).

Toxicity of anti-TB drug candidates under clinical development has been one of the major setbacks in TB research. The TB alliance recently announced the discontinuation of TBA-354 from Phase 1 clinical trials due to participants displaying mild signs of neurotoxicity [15, 16]. The observed signs were, the involuntary movement of the eyes and overactive reflexes [16]. In drug development studies, it is important to understand the drug's pharmacokinetics and distribution in different biological systems. Liquid chromatography-tandem mass spectrometry (LC-MS/MS) is one of the major analytical techniques used to quantify the total drug concentration from target organs, but it is disadvantaged in that it cannot provide spatial information regarding drug distribution. Drugs under development must be studied for their blood-brain barrier (BBB) permeability before clinical trials to avoid central nervous system (CNS) side effects and possible neurotoxicity. When evaluating the safety of the drug, knowing its specific location is an important aspect in drug development and molecular imaging techniques are normally used to evaluate specific drug localization. Well recognized techniques such as magnetic resonance imaging (MRI) and positron emission tomography (PET) are commonly used for molecular imaging. However, these techniques often require the radioactive labeling of a target compound to ease the mapping process, [17] in addition to being expensive [18]. Matrix-assisted laser desorption/ionization-mass spectrometry imaging (MALDI-MSI) is an emerging technique used for direct analysis of compounds from tissue samples without radioactive labeling [19, 20]. Previously, we successfully used MSI to investigate the distribution of several anti-TB drugs in brain [21-24] including pretomanid [13].

Therefore, in this study we focused on the development of mass spectrometric methods to understand the preclinical pharmacokinetics and spatial distribution of TBA-354 via a validated quantitative liquid chromatography-tandem mass spectrometry (LC-MS/MS) method and matrix-assisted laser desorption/ionization-mass spectrometric imaging (MALDI-MSI), respectively.

2.4. Materials and methods

2.4.1. Materials and reagents

TBA-354 was acquired from DLD scientific (Durban, South Africa). Pretomanid (internal standard), was obtained from Sigma-Aldrich (Germany). LC-MS grade methanol (MeOH) and acetonitrile (ACN) were purchased from Sigma-Aldrich. Analytical grade formic acid (FA) was purchased from Merck Millipore (Merck, South Africa). α-cycno-4-hydroxy-cinnamic acid (HCCA) was purchased from Bruker. A Milli-Q purification system (Bedford, MA, USA) was used for the preparation of ultrapure water. Solid-phase extraction (SPE) cartridges; Supel™ - Select HLB SPE (30 mg, 1 mL), Discovery® DSC-PS/DVB SPE C_{18} (50 and 100 mg, 1 mL), and HybridSPE-Phospholipid (30 mg, 1 mL) was purchased from Supelco-Sigma (St. Louis, MO). All other chemicals used in this study were of analytical grade.

2.4.2. LC-MS/MS method

The liquid chromatography (LC) system was Agilent technologies 1100 (Agilent, Germany) series liquid chromatography coupled to a Bruker QTOF-II (Bruker Daltonics, Bremen, Germany) with electrospray ionization (ESI) source and a time-of-flight mass spectrometry (TOF-MS) mass analyzer (Bruker Daltonics, Bremen, Germany). Analysis 4.0 SP 5 (Bruker Daltonics) was used to further process the data.

Chromatographic separation was achieved using a YMC Triart C_{18} Column (150.0 mm x 3.0 mm; 3.0 µm particle size) (YMC Europe GmbH, Dislanken, Germany) coupled to a compatible 4.0 mm x 3.0 mm guard cartridge. Mobile phase A was ultra-pure water (0.1% v/v FA) and mobile phase B was ACN (0.1% v/v FA), with a flow rate of 0.4 ml/min and column compartment was set to room temperature. A gradient method was used to achieve chromatographic separation, it was initially increased from 50 to 70% B for 10 min, held for 2 min thereafter it was returned to 50% B over 5 min, re-equilibration time was 5 min.

The MS acquisition parameters were: ion polarity was positive, end plate offset was 500 V, capillary voltage was 4500 V, nebulizer was 1.5 bar, dry gas flow rate was 8 l/min, dry heater temperature was 200 ^{o}C, scan range was from *m/z* 100 to 600, collision cell radiofrequency was 500 Vpp and collision energy was 30 eV for TBA-354 and 13 eV for the IS.

2.4.3. Biological samples

Blank plasma lung and brain samples were obtained from untreated Sprague-Dawley rats. The lung and brain samples were weighed and cut into smaller pieces using a surgical scalpel blade and then homogenized in ultra-pure water (3 mL/g tissue). All lung, brain homogenates and plasma samples were stored at -80 ◦C until analysis.

2.4.4. Preparation of standards and quality control samples

The 100 µg/ml stock solutions of TBA-354 and the internal standard (IS) were prepared separately in MeOH and stored at -20 ºC where they were found to be stable. A series of TBA-354 working standard solutions were prepared by diluting the stock solution using the extraction solvent (ACN or MeOH) along with the IS working standard solution at 5 µg/ml. For calibration standards, 100 µL of blank samples from untreated Sprague-Dawley rats were spiked with working standard solutions of TBA-354 (50 µL) and the IS (50 µL). The TBA-354 concentrations were starting from 20 to 1500 ng/mL, 25 to 1400 ng/g, 10 to 1400 ng/g for plasma, lung and brain homogenates, respectively with the IS kept at 250 ng/mL in each sample. Following the same procedure, four quality control (QC) samples were investigated, including the lower limit of quantification (LLOQ), low-quality control (LQC), middle-quality control (MQC) and high-quality control (HQC) samples.

2.4.5. Sample preparation and optimization

During sample preparation, 100 µL of the biological sample was spiked 100 µL of IS to yield 250 ng/mL and vortexed for 1 min after which 800 µL of ACN (for lung and brain homogenates) or MeOH (for plasma homogenate) was added to extract target analytes while inducing the precipitation of proteins from the biological samples. The mixture was then vortexed for 1 min then followed by centrifugation at 13 000 *g* for 15 min at 4 ºC. The supernatants were filtered through an SPE cartridge suitable for each biological. The selection of SPE cartridges was based on the recoveries of the target analyte after filtration. The filtrate was then collected into the auto-sampler vials and vortexed briefly, before the injection of 5 µL into the LC-MS/MS system.

2.4.6. Method validation procedures

The method used in this study was validated according to the EMA guidelines on bioanalytical method validation [25]. Validation parameters covered in this study include specificity, selectivity, linearity, LLOQ, accuracy, precision, matrix effect, recovery, and the stability.

2.4.6.1. Specificity and selectivity

The experiments conducted to evaluate the specificity and selectivity of the method involved comparison of the chromatograms from six different sets of blank biological samples obtained from six different sources. Each blank biological sample was tested under the LC-MS/MS conditions mentioned above to evaluate if there were any interfering peaks at the retention times of TBA-354 and the IS. Possible interferences may come from endogenous compounds in the biological sample.

2.4.6.2. Linearity and LLOQ

The calibration curves for quantification of TBA-354 in rat biological samples were constructed by plotting the peak area ratio of analyte to IS against the theoretical concentrations of the analyte, using $1/x^2$ weighted linear regression. The LLOQ was defined as the lowest quantifiable concentration in the calibration range with a minimum signal-to-noise (S/N) ratio of 5:1.

2.4.6.3. Accuracy and precision

The evaluation of intra-day and inter-day precision and accuracy involved analysis of four QC samples (LLOQ, LQC, MQC, and HQC) in six replicates. For plasma, QC levels were 20, 50, 750 and 1400 ng/mL, for lung homogenate were 25, 75, 750 and 1300 ng/g and 10, 30, 600 and 1200 ng/g for brain homogenate. QC samples were analyzed against the calibration curve, and the obtained concentrations were compared to the nominal concentration values. Accuracy and precision were expressed in terms of percentage of concentration found to the nominal concentration and percentage relative standard deviation (% RSD), respectively. According to EMA guidelines, the mean concentration should be within ± 15% of the nominal concentration value for the QC sample, except for the LLOQ which should be within ± 20% of the nominal concentration value [25].

2.4.6.4. Matrix effect and extraction recovery

Using ACN or MeOH as an extraction solvent, four different SPE cartridges were tested and the one that produced acceptable recoveries was selected. Matrix effect was tested for six different lots of drug-free rat plasma, and lung homogenates. The matrix effect for each lot was evaluated at LQC, MQC, and HQC (n = 6). The average peak ratio of the analyte for each spiked sample was then compared to the average peak ratio of the analytical standard solution at the same concentration. According to EMA guidelines, the variability of matrix factor should be within ± 15% [25]. The extraction recovery of TBA-354 was determined by comparing the peak ratios from the extracted samples with the peak ratios from un-extracted samples at LQC, MQC, and HQC concentration levels (n = 6).

2.4.6.5. Stability

The stability of a drug in biological samples depends on the chemical and physical properties of the drug, storage conditions and the matrix effect [26]. The stability of TBA-354 in rat plasma, lung and brain homogenate samples was determined at three QC levels with each QC sample analyzed in six replicates. The short-term stability was studied by keeping the samples in a bench-top at room temperature for a period of 6 h. Freeze-thaw stability was evaluated after three freeze-thaw cycles. The post-preparation stability

was evaluated by analyzing the extracted samples stored in the auto-sampler for a period of 24 h before analysis.

2.4.7. Animal study

All animal study experiments were approved by the Animal Research Ethics Committee (AREC) of the University of KwaZulu-Natal (UKZN) (approval reference: 006/016M). Female Sprague-Dawley rats (weighted 120 ± 20 g) obtained from Biomedical Resource Unit (UKZN, Durban, South Africa), were housed under standard conditions, in an air-conditioned room with a 12 h light/dark cycle and were given *ad libitum* access to food and water.

2.4.7.1. Drug administration and sample collection

TBA-354 was prepared in a 10% (v/v) aqueous solution of dimethyl sulfoxide (DMSO). Female Sprague-Dawley rats (weight of 120 ± 20 g) were administered 20 mg/kg of TBA-354 aqueous solution *via* i.p. injection. Animals were anesthetized with halothane overdose before sacrifice. Termination of animals was done at 0.25, 0.5, 1, 2, 4, 6, 8, and 24 h (n = 3 per time point). The cardiac puncture technique was used during the blood sample collection. Blood samples were immediately transferred into the K_3-EDTA-coated tubes and centrifuged at 10 000 *g* for 10 min, and plasma was collected and stored at -80 ^{o}C until the analysis. Tissue samples were frozen using liquid nitrogen and then stored at -80 ^{o}C until the analysis.

2.4.8. MALDI-MSI sample preparation

Sectioning of the rat brain was done using a Leica Microsystems CM1100 (Wetzlar, Germany) cryostat set at -20 ◦C. Brain tissues with the thickness of 12 µm were sectioned and thaw-mounted onto indium titanium oxide (ITO)-coated slides (Bruker Daltonics, Bremen, Germany). The samples were air-dried for 25 min at room temperature and then stored under inert conditions in the desiccator for 24 h. The matrix was a mixture comprised of 7 mg/mL HCCA dissolved 15% H_2O, 85% ACN and 0.1% FA. The mixture was sonicated for 15 minutes and spray-coated onto the slides using the ImagePrep.

2.4.9. MSI analysis

All MSI experiments were conducted on an UltrafleXtreme MALDI-TOF/TOF MS system (Bruker Daltonics, Bremen, Germany). MS and MS/MS data were gathered in positive ion mode within the mass range of *m/z* 200 to 600. Each pixel was collected using 1500 individual laser shots per spectrum. Images were acquired using a raster width of 70 µm.

2.5. Results and discussion

2.5.1. LC-MS/MS method development and optimization

The chromatographic separation of TBA-354 and the IS was achieved using a binary gradient mobile phase of ultrapure water (0.1% FA) and ACN (0.1% FA). The retention time of TBA-354 was 6.5 min and that of the IS was 5.9 min. The positive ion mode showed a better signal of the target analyte when compared to negative ion mode. The addition of 0.1% FA improved the intensity of the analyte's signal by protonating the target analytes into protonated adducts. Precursor and product ions were determined by injecting 500 ng/ml solutions into the MS using in the range of *m/z* 100 to 600. The MS spectra for the target analyte and IS showed the presence of the protonated precursor [M+H] positive ions at *m/z* 437.1 and 360.1 for TBA-354 and IS, respectively. The mass spectrometer was used in positive ion mode to monitor the mass transitions of TBA-354 and IS, multiple reaction monitoring (MRM) mode was selected. Optimum MRM parameters were: isolation width of 5 for both target analyte and IS and the collision energy of 30 eV for TBA-354 and 13 eV for the IS. For quantification purposes, the most intense transition was chosen *m/z* 437.1 $\rightarrow$ 252.1 for TBA-354 and *m/z* 360.1 $\rightarrow$ 330.1 for IS. MRM chromatograms and their corresponding MS spectra for both IS and TBA-354 are shown in **Figure 2.2**.

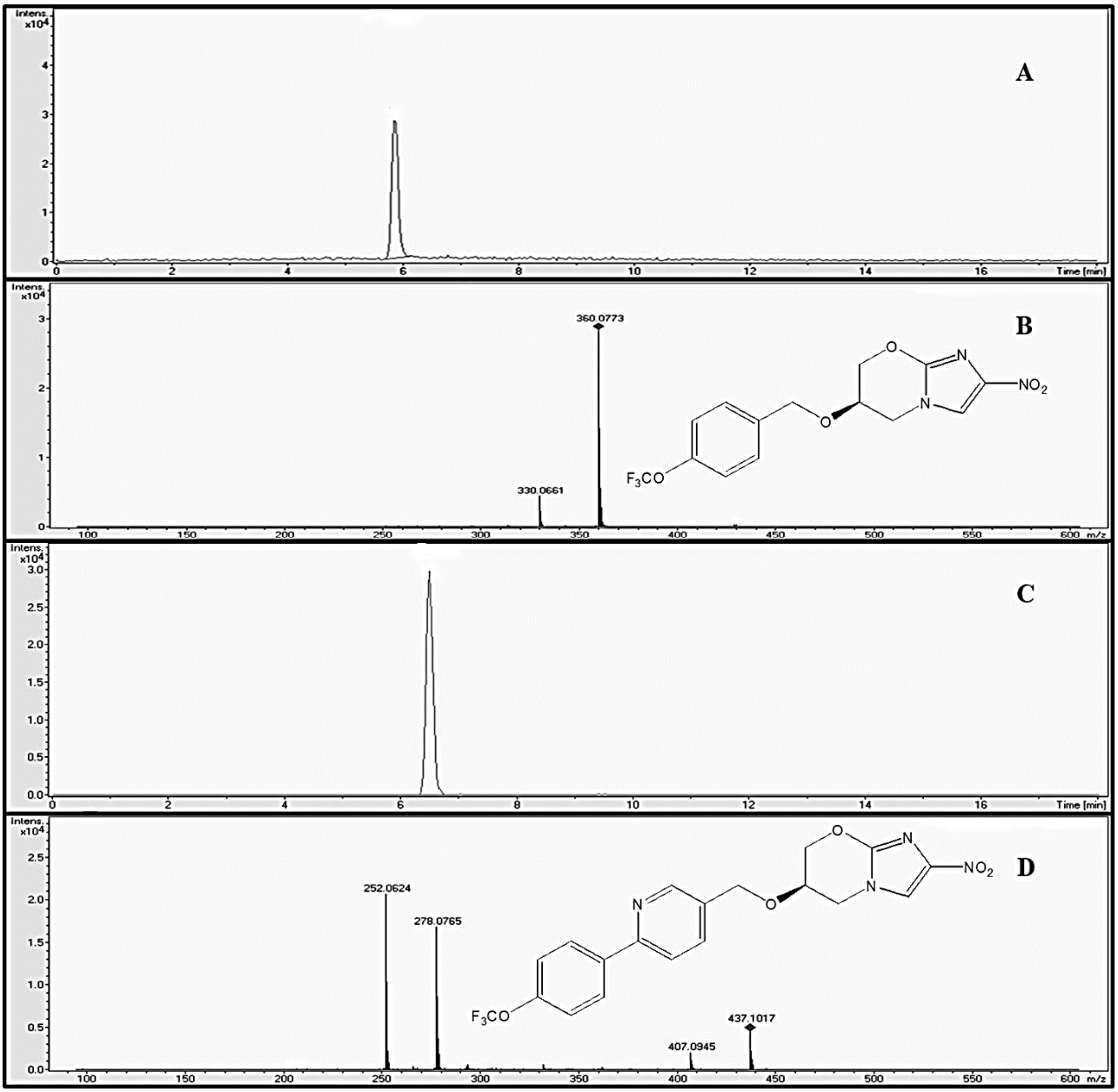

Figure 2.2. MRM chromatograms and mass spectrums for TBA-354 (500 ng/mL) and IS (250 ng/mL) in plasma samples. (A) chromatogram for IS, (B) MRM transition of *m/z* 360.1 → 330.1 for IS, (C) chromatogram for TBA-354 and (D) MRM transition of *m/z* 437.1 → 252.1 for TBA-354.

2.5.2. Sample extraction method development and optimization

SPE is used as a clean-up to remove endogenous substances from biological matrices, which may affect the analysis. Recoveries were determined by using different cartridges and solvents (MeOH or ACN), as protein precipitants. The best recoveries were achieved using the Discovery® DSC-PS/DVB SPE C_{18} (100

mg, 1 mL) and MeOH for plasma, and HybridSPE-Phospholipid (30 mg, 1 mL) and ACN for lung homogenate and Supel™ - Select HLB (30 mg, 1 mL) and ACN for brain homogenate.

2.5.3. Method validation

2.5.3.1. Specificity and selectivity

The detection of TBA-354 (retention time = 6.5 min) and IS (retention time = 5.9 min) was highly selective and there were no interfering endogenous substances at the retention time. The results confirmed that the method is selective for the analysis of TBA-354 in rat plasma lung and brain homogenates.

2.5.3.2. Linearity and LLOQ

Linear responses for TBA-354 ranged from 20 to 1500 ng/mL ($y = 0.235334 x + -0.005533$, $R^2 = 0.999597$), 25 to 1400 ng/mL ($y = 0.543408 x + 0.003964$, $R^2 = 0.999762$) and 10 to 1400 ng/mL ($y = 0.373539 x + 0.015013$, $R^2 = 0.999533$) in plasma, lung and brain homogenates, respectively, where y is the peak area ratio of the analyte to the IS and x represents the concentration of TBA-354. The lower limit of quantification (LLOQ), determined using a signal to noise ratio of ≥5, was 20 ng/mL, 25 ng/g and 10 ng/g for plasma, lung and brain homogenate respectively.

2.5.3.3. Recovery and matrix effect

Biological samples such as plasma, lung and brain homogenates contain endogenous substances (proteins, phospholipids, etc.) which may affect the analysis and some of them may be co-extracted with the target analyte during the extraction process. Thus, they must be removed from the sample prior analysis. Two different techniques were used to eliminate endogenous substances, protein precipitation and SPE. Protein precipitation technique can effectively remove proteins but it cannot remove all endogenous substances. Therefore, SPE was used as an additional technique to remove phospholipids and other substances.

Matrix effect is defined as the effect on an analytical method caused by other unwanted components of the sample except the target analyte to be quantified [27]. The matrix effect of endogenous compounds on the recovery of blank biological samples spiked, after the sample preparation at three QC levels (LQC, MQC and HQC) of the analyte were found to be within the limits set by EMA guidelines. The matrix factor ranged from -4.72 to -1.34% and the recoveries ranged from 91.07 to 97.39%. This confirmed that the matrix effect from the biological samples investigated was negligible in this study (**Table 2.1**).

Table 2.1. Extraction recovery and matrix effects of TBA-354 in different biological samples.

Sample	QC level	Mean recovery (%)	% RSD	Matrix effect (%)	% RSD
Plasma					
	Low	94.29	1.95	-3.34	1.55
	Middle	96.21	2.31	-2.71	2.67
	High	97.39	1.76	-4.72	1.31
Lungs					
	Low	94.81	3.44	-1.34	1.28
	Middle	91.07	2.19	-2.07	1.46
	High	95.86	1.92	-1.45	1.23
Brain	Low	87.50	7.27	-6.31	8.27
	Middle	94.92	3.36	-3.78	1.34
	High	93.74	2.10	-4.26	2.71

2.5.3.4. Accuracy and precision

The intra-day accuracy and precision were determined using six replicates of individual QC levels within the same day. Inter-day variability was evaluated as the accuracy and precision of the mean QC concentrations (LLOQ, LQC, MQC and HQC) on three consecutive days. For intra-day evaluation, % RSD varied from 0.38 to 3.05%, and the accuracy varied from 90.76 to 97.95% of nominal concentrations. For inter-day evaluation, % RSD varied from 0.40 to 2.02% and the accuracy varied from 91.67 to 97.59% of nominal concentrations. Intra-day and inter-day accuracy and precision data for the method validation study are presented in **Table 2.2**. All the values were found to be within variability limits set by EMA [25].

Table 2.2. Accuracy and precision of the method for TBA-354 in biological samples.

Sample	Parameter	LLOQ	LQC	MQC	HQC
Plasma	Nominal concentration (ng/mL)	20.00	50.00	750.00	1400.00
	Intra-day (n = 6)				
	Average concentration found	19.30	48.46	725.85	1366.29
	Accuracy (%)	96.52	96.91	96.78	97.59
	% RSD	1.97	1.95	2.71	3.05
	Inter-day (n = 6)				
	Average concentration found	19.42	47.88	718.49	1365.01
	Accuracy (%)	97.08	95.76	95.80	97.50
	% RSD	1.17	1.23	2.02	0.66
Lungs	Nominal concentration (ng/g)	25.00	75.00	750.00	1300.00
	Intra-day (n = 6)				
	Average concentration found	23.44	71.17	693.11	1179.86
	Accuracy (%)	93.75	94.89	92.41	90.76
	% RSD	0.41	0.51	0.38	0.93
	Inter-day (n = 6)				
	Average concentration found	23.38	70.95	693.21	1191.71
	Accuracy (%)	93.53	94.60	92.43	91.67
	% RSD	0.96	0.40	0.44	1.15
Brain	Nominal concentration (ng/g)	10.00	30.00	600.00	1200.00
	Intra-day (n = 6)				
	Average concentration found	10.17	27.40	537.17	1073.24
	Accuracy (%)	101.73	91.33	89.53	89.44
	% RSD	4.92	2.40	2.78	2.10
	Inter-day (n = 6)				
	Average concentration found	9.96	27.59	535.32	1089.33
	Accuracy (%)	99.61	91.97	89.22	90.78
	% RSD	1.95	0.69	0.35	2.09

2.5.3.5. Stability

The QC samples spiked with TBA-354 were analyzed for stability at different storage conditions. The concentrations are shown in **Table 2.3** with the corresponding accuracy (%) and precision (% RSD). According to the stability study conducted, TBA-354 is stable in any one of the conditions that were investigated since the mean concentration at each QC level was within ±15% of the nominal concentration.

Table 2.3. Stability of TBA-354 in different rat biological samples (n = 6).

Sample	Nominal concentration (ng/mL or ng/g)	Storage condition					
		Bench top for 6 h (RT)		Auto-sampler, 24 h		Three freeze/thaw cycles	
		Accuracy (%)	% RSD	Accuracy (%)	% RSD	Accuracy (%)	% RSD
Plasma	50.00	93.49	5.72	94.93	1.28	95.82	7.40
	750.00	92.49	4.10	93.25	1.00	90.35	4.15
	1400.00	94.75	5.57	90.79	1.19	85.70	5.88
Lungs	75.00	93.00	0.54	95.25	0.60	90.73	0.89
	750.00	89.23	1.04	90.87	1.47	88.84	0.95
	1300.00	90.43	1.14	92.38	0.86	92.79	0.63
Brain	30.00	92.53	0.72	102.81	1.21	99.39	5.15
	750.00	90.39	3.83	86.87	1.49	88.68	1.68
	1200.00	93.13	6.57	94.08	0.36	92.51	0.78

RT = room temperature

2.5.4. Pharmacokinetics and tissue distribution study

LC-MS/MS method was validated and then applied to the investigation of the plasma pharmacokinetics, lung and brain distribution of TBA-354 after single i.p. administration of 20 mg/kg in Sprague-Dawley rats. The PK and tissue distribution parameters for TBA-354 in plasma, lung and brain homogenates are summarized in **Table 2.4**.

In plasma samples, the drug could only be quantified from 0.25 to 8.00 h. However, after 24.00 h traces of TBA-354 were detected, but the concentrations were below the limit of quantification. Following i.p. administration, the drug in rat plasma reached the maximum concentration (C_{max}) of 2048.76 ng/mL and the time it took to reach the maximum concentration (T_{max}) was 6.00 h. The terminal half-life ($t_{1/2}$) of TBA-354 in plasma was 2.24 h. The drug exposure was defined as the area under the curve from time zero to the last time-point with the quantifiable concentration (AUC_{0-t}) [28] and it was 10134.73 ng. h/mL. The pharmacokinetic profile for TBA-354 after an i.p. single dose administration of 20 mg/kg, showed that the absorption of the drug gradually increased until it reached the C_{max}, then followed by a rapid elimination, see **Figure 2.3**.

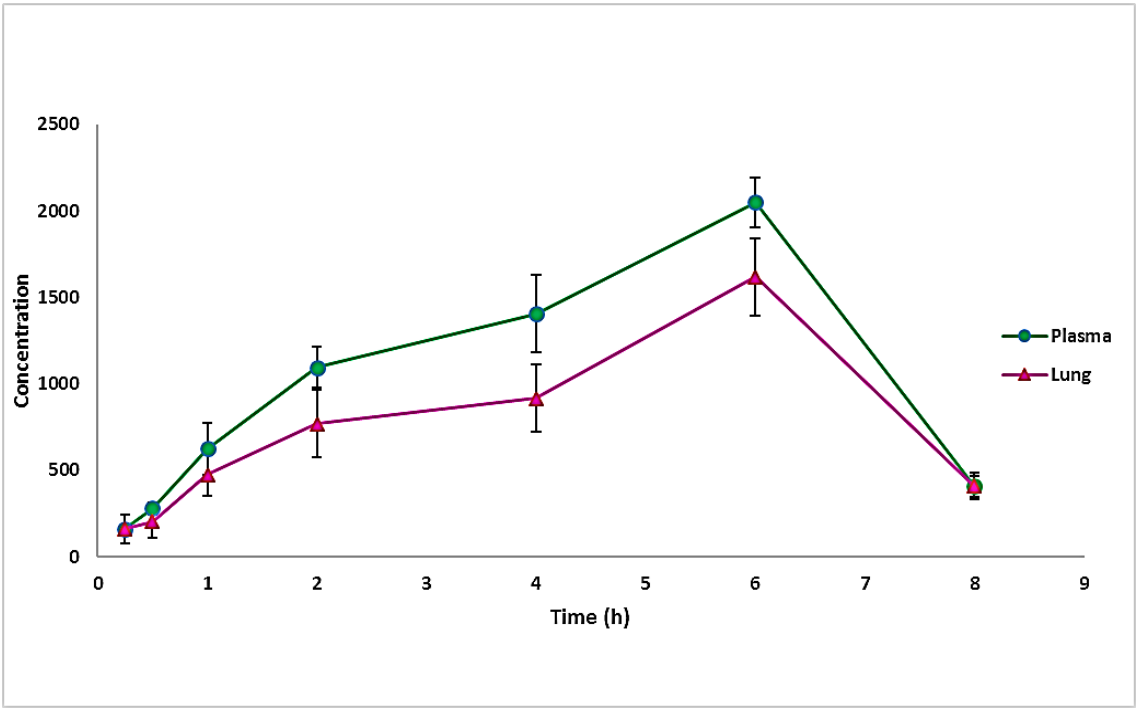

Figure 2.3. Concentration-time profiles of plasma (ng/mL) and lung homogenate (ng/g) for TBA-354 after a single dose of 20 mg/kg to the rats *via* i.p. administration (data is represented as a mean ± SD).

The lung concentration-time profile for TBA-354 after an i.p. single dose administration of 20 mg/kg is presented in **Figure 2.3**. For the lung homogenate samples, the drug was only quantifiable from 0.25 to 8.00 h. At 24.00 h post dose, the drug concentration was below the limit of quantification. The drug had a C_{max} of 1617.98 ng/g, T_{max} of 6.00 h, and $t_{1/2}$ of 7.40 h. AUC_{0-t} was found to be 7530.59 ng h/g. The lung homogenate samples had lower concentrations of TBA-354 compared to plasma samples. The calculated AUC_{0-t} plasma to lung ratio was 74.30%.

The brain concentration-time profile for TBA-354 after an i.p. administration is shown in **Figure 2.5**. TBA-354 managed to enter the central nervous system (CNS) and cross the blood-brain barrier (BBB) and was detected after 0.25 h in the brain. The quantifiable concentrations were of samples obtained at 0.50 to 8.00 h. After 24.00 h, traces of TBA-354 were detected but non-quantifiable. TBA-354 reached the C_{max} of 713.36 ng/g at T_{max} of 6.00 h. The $t_{1/2}$ of TBA-354 in the brain was 3.30 h and the AUC_{0-t} was 3332.97 ng h/g. The brain homogenate samples had lower concentrations of TBA-354 compared to plasma samples. The AUC_{0-t} plasma/brain ratio was 32.89%.

Table 2.4. Pharmacokinetic parameters of TBA-354 in rats following a single dose i.p. administration of 20 mg/kg.

Parameter	Plasma	Lung	Brain
C_{max} ± SD (ng/mL or ng/g)	2048.76 ± 143.60	1617.98 ± 233.59	713.36 ± 119.67
T_{max} (h)	6.00	6.00	6.00
$t_{1/2}$ (h)	2.24	3.43	3.30
AUC_{0-t} (ng h/mL or ng h/g)	10134.74	7530.59	3332.97

2.5.5. MSI

One of the major challenges in drug development is to find a method to monitor the drug movement through the CNS, BBB permeability and its localization in the brain without the requirement of molecular labeling. As explained above, the drug could easily penetrate the BBB. This study demonstrates the use of MSI to visualize and localize traces of TBA-354 that were able to penetrate the BBB and enter the brain, where it exerts its neurotoxic effects.

The MSI method was optimized for the detection of TBA-354 on brain tissue samples. The $[M + H]^+$ ion of *m/z* 437.1 and the fragments, *m/z* 252.1 and 278.1 ions were monitored during the mapping of TBA-354 in brain tissue sections (**Figure 2.4** and **2.5**). To acquire mass spectral images, a tissue section is coated

with the matrix forming a homogeneous layer on top of the tissue. The laser is rastered transversely on the tissue surface, and spectra are acquired from each spot.

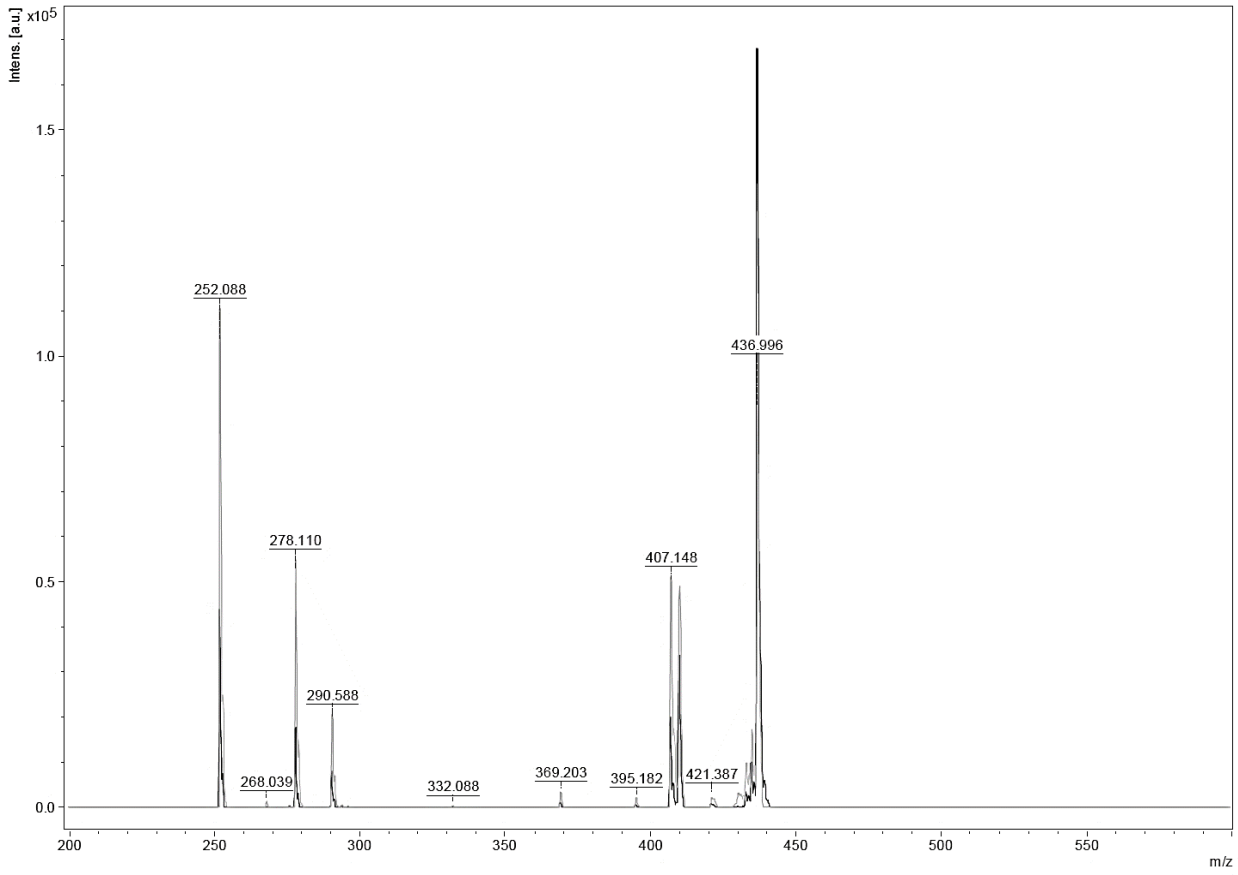

Figure 2.4. Typical MALDI-MSI spectrum for TBA-354 acquired in the MS/MS mode where the $[M + H]^+$ ion of *m/z* 437.1 ± 0.2 and the fragments 252.1 ± 0.2 and 278.1 ± 0.2 were monitored for imaging.

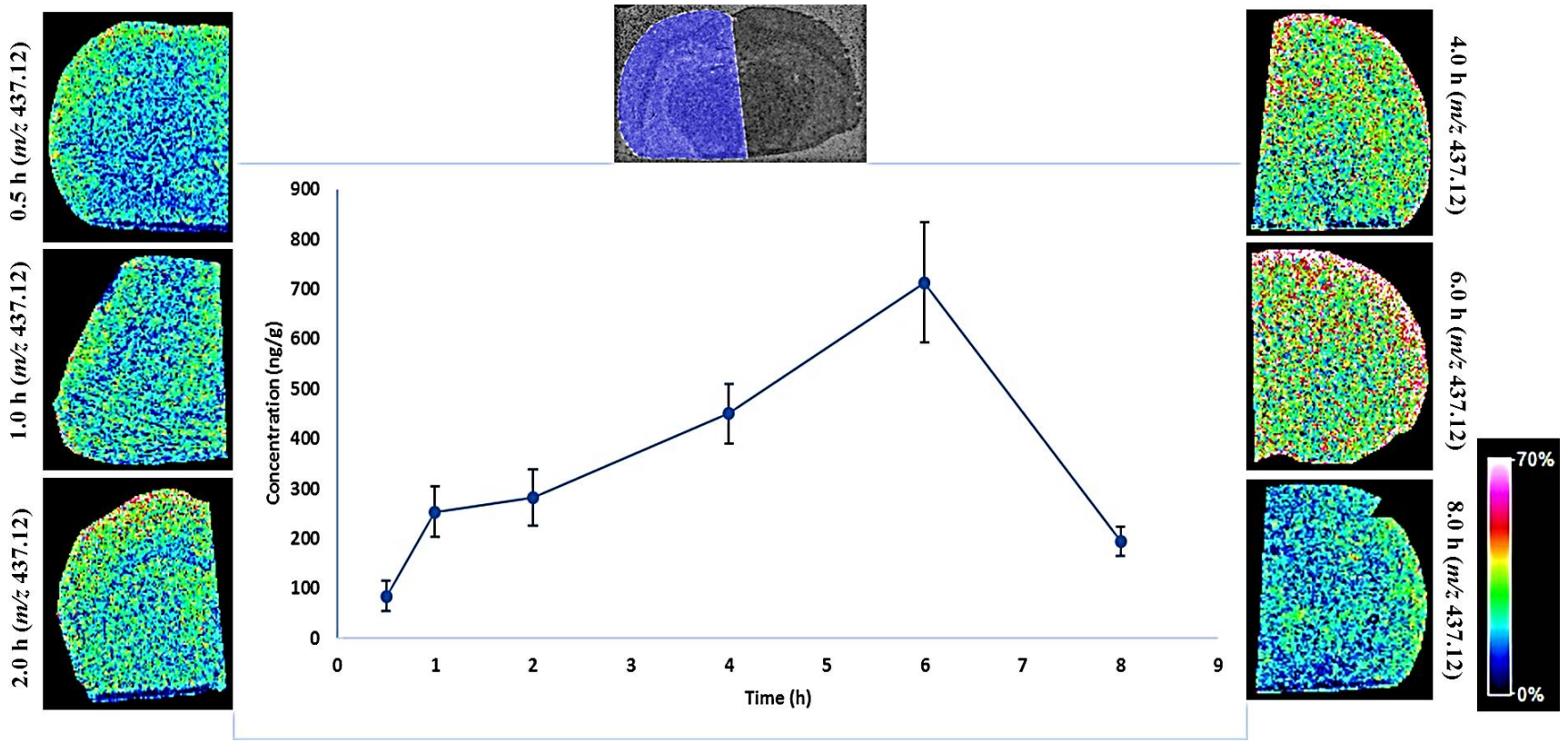

Figure 2.5. Brain concentration-time profile for TBA-354 after a single dose of 20 mg/kg to the rats *via* i.p. administration (data is represented as a mean ± SD) and the corresponding MSI images showing the drug distribution in coronal brain sections. The images shown here were obtained from 0.50 to 8.00 h, using MS/MS mode monitoring the $[M + H]^+$ ion of *m/z* 437.1 and *m/z* 252.1 and 278.1 fragment ions. Images representing 0.50 to 6.00 h showed the gradual increase of the *m/z* 437.1 ion distributed mostly in the neocortex. From 6.00 to 8.00 h there was a rapid elimination of the drug as reflected by the 8.00 h image displaying low intensity of the *m/z* 437.1 ion.

Using MSI to investigate the localization of the drug in rat brain, the parent ion (*m/z* 437.1) was detected in from the sections obtained from 0.50 up to 8.00 h postdose. The MSI images showed that the drug penetration through the BBB gradually increased from 0.5 h reaching the C_{max} at 6.00 h postdose and the rapid elimination of the drug from the brain with low intensity displayed at 8.00 h (**Figure 2.5)**. The drug could not be detected at 0.25 and 24 h. The quantitative LC-MS/MS results also showed the C_{max} at 6.00 h postdose, which corresponds to the imaging results with the highest intensity seen at the same time point. At 6.00 h postdose, the drug was distributed homogeneously throughout the regions of the brain, with high levels of the drug accumulating in the neocortex, a part of the cerebral cortex involved in the visual, hearing and motor systems in mammals which explains the neurotoxic signs (repetitious involuntary eye movement), observed during TBA-354 clinical trials [16]. We have previously investigated the distribution of pretomanid (a drug in the same class as TBA-354) in rat brain and our findings demonstrated that the drug does cross the BBB and accumulates in the corpus callosum which is different from the distribution of TBA-354 [13].

The balance between the activity and toxicity of any drug is required in pre-clinical and clinical drug development in order to avoid unnecessary costs. From the results, it shows that the imbalance between an anti-TB activity and the toxicity of TBA-354 is unacceptable, which is an unfortunate circumstance that led to the termination of this drug's clinical trials.

2.6. Conclusions

In this study, we have developed and validated sensitive and reproducible mass spectrometric methods for the pharmacokinetics of TBA-354 in rat plasma, lung and brain homogenate samples as well as for its spatial distribution in brain. This study has shown that even though TBA-354 has an excellent anti-TB activity, there are high risks associated with its use due to its high BBB permeability, resulting in the accumulation of toxic levels of the compound which leads to unacceptable neurotoxic side effects. By comparing the distribution of TBA-354 with previous MSI analysis of pretomanid's drug distribution in the brain, we can prove that different drugs from the same class of compounds can display varied localization patterns.

2.7. Acknowledgements

Authors would like to thank the whole Catalysis and Peptide Research Unit (CPRU) team for the support.

2.8. Funding

This work was supported by the National Research Foundation, Medical Research Council, Aspen Pharmacare and the University of KwaZulu-Natal, Durban.

2.9. Transparency declarations

None to declare

2.10. References

1. World Health Organization. *Global tuberculosis report*, 2016. [cited 2016 21 October]; Available from: http://apps.who.int/iris/bitstream/10665/250441/1/9789241565394-eng.pdf?ua=1.
2. Mugunthan, G., et al., *Synthesis and screening of galactose-linked nitroimidazoles and triazoles against Mycobacterium tuberculosis.* European Journal of Medicinal Chemistry, 2011. **46**: p. 4725-4732.
3. Barry, C.E., et al., *The spectrum of latent tuberculosis: rethinking the goals of prophylaxis.* Nature reviews. Microbiology, 2009. **7**: p. 845-855.
4. López-Gavín, A., et al., *In vitro activity against Mycobacterium tuberculosis of levofloxacin, moxifloxacin and UB-8902 in combination with clofazimine and pretomanid.* International Journal of Antimicrobial Agents, 2015. **46**: p. 582-585.
5. Wang, L., et al., *LC–MS/MS method for the simultaneous determination of PA-824, moxifloxacin and pyrazinamide in rat plasma and its application to pharmacokinetic study.* Journal of Pharmaceutical and Biomedical Analysis, 2014. **97**: p. 1-8.
6. Meng, M., et al., *Simultaneous quantitation of delamanid (OPC-67683) and its eight metabolites in human plasma using UHPLC–MS/MS.* Journal of Chromatography B, 2015. **1002**: p. 78-91.
7. Lee, S.J., et al., *Development and validation of LC-ESI-MS/MS method for analysis of moxifloxacin and levofloxacin in serum of multidrug-resistant tuberculosis patients: Potential application as therapeutic drug monitoring tool in medical diagnosis.* Journal of Chromatography B, 2016. **1009**: p. 138-143.
8. Khan, A., S. Sarkar, and D. Sarkar, *Bactericidal activity of 2-nitroimidazole against the active replicating stage of Mycobacterium bovis BCG and Mycobacterium tuberculosis with intracellular efficacy in THP-1 macrophages.* International Journal of Antimicrobial Agents, 2008. **32**: p. 40-45.
9. Cavalleri, B., et al., *New 5-substituted 1-alkyl-2-nitroimidazoles.* Journal of Medicinal Chemistry, 1973. **16**: p. 557-560.
10. Manjunatha, U., H.I.M. Boshoff, and C.E. Barry, *The mechanism of action of PA-824: Novel insights from transcriptional profiling.* Communicative & Integrative Biology, 2009. **2**: p. 215-218.
11. Ryan, N.J. and J.H. Lo, *Delamanid: First Global Approval.* Drugs, 2014. **74**: p. 1041-1045.

12. Bratkowska, D., et al., *Determination of the antitubercular drug PA-824 in rat plasma, lung and brain tissues by liquid chromatography tandem mass spectrometry: Application to a pharmacokinetic study.* Journal of Chromatography B, 2015. **988**: p. 187-194.

13. Shobo, A., et al., *Tissue distribution of pretomanid in rat brain via mass spectrometry imaging.* Xenobiotica, 2016. **46**: p. 247-252.

14. Upton, A.M., et al., *In Vitro and In Vivo Activities of the Nitroimidazole TBA-354 against Mycobacterium tuberculosis.* Antimicrobial Agents and Chemotherapy, 2015. **59**: p. 136-144.

15. TB-Alliance. *Phase 1 Clinical Trial of TB Drug Candidate TBA-354 Discontinued*, 2016. [cited 2016 20 May]; Available from: http://www.tballiance.org/news/phase-1-clinical-trial-tb-drug-candidate-tba-354-discontinued.

16. i-Base. *The tuberculosis treatment pipeline: activity, but no answers*, 2016. [cited 2016 04 October]; Available from: http://i-base.info/htb/30164

17. Rohner, T.C., D. Staab, and M. Stoeckli, *MALDI mass spectrometric imaging of biological tissue sections.* Mechanisms of Ageing and Development, 2005. **126**: p. 177-185.

18. Shobo, A., et al., *MALDI MSI and LC-MS/MS: Towards preclinical determination of the neurotoxic potential of fluoroquinolones.* Drug Testing and Analysis, 2016. **8**: p. 832-838.

19. Andersson, M., et al., *Imaging mass spectrometry of proteins and peptides: 3D volume reconstruction.* Nat Meth, 2008. **5**: p. 101-108.

20. Chan, K., et al., *MALDI mass spectrometry imaging of gangliosides in mouse brain using ionic liquid matrix.* Analytica Chimica Acta, 2009. **639**: p. 57-61.

21. Baijnath, S., et al., *Evidence for the presence of clofazimine and its distribution in the healthy mouse brain.* Journal of Molecular Histology, 2015. **46**: p. 439-442.

22. Baijnath, S., et al., *Neuroprotective potential of Linezolid: a quantitative and distribution study via mass spectrometry.* Journal of Molecular Histology, 2016. **47**: p. 429-435.

23. Shobo, A., et al., *MALDI MSI and LC-MS/MS: Towards preclinical determination of the neurotoxic potential of fluoroquinolones.* Drug Testing and Analysis, 2015. **8**: p. 832-838.

24. Shobo, A., et al., *Visualization of Time-Dependent Distribution of Rifampicin in Rat Brain Using MALDI MSI and Quantitative LCMS/MS.* ASSAY and Drug Development Technologies, 2015. **13**: p. 277-284.

25. E.M.A. *European Medicines Agency, C.H.M.P. Committee for Medicinal Products for Human Use*, 2009. [cited 2016 15 March]; Available from:

http://www.ema.europa.eu/docs/en_GB/document_library/Scientific_guideline/2011/08/WC500109686.pdf.

26. Kour, G., et al., *Development and validation of a highly sensitive LC–MS/MS-ESI method for quantification of IIIM-019—A novel nitroimidazole derivative with promising action against Tuberculosis: Application to drug development.* Journal of Pharmaceutical and Biomedical Analysis, 2016. **124**: p. 26-33.

27. Smeraglia, J., S.F. Baldrey, and D. Watson, *Matrix effects and selectivity issues in LC-MS-MS.* Chromatographia, 2002. **55**: p. S95-S99.

28. Roos, J.F., et al., *Pharmacokinetic-pharmacodynamic rationale for cefepime dosing regimens in intensive care units.* Journal of Antimicrobial Chemotherapy, 2006. **58**: p. 987-993.

Chapter 3

General discussion and conclusions

3.1. General discussion and conclusions

Tuberculosis (TB) remains the major cause of death in humans and people living with HIV are the most vulnerable, due to co-infection. The world is facing a challenge of dealing with multidrug-resistant (MDR), extensively drug-resistant (XDR) TB and HIV-TB co-infection. Unfortunately, the available anti-TB drugs for MDR-TB or XDR-TB are in short supply and expensive, with many of them experiencing drug resistance. Although there has been an improvement in the current regimens used for the treatment of TB in terms of complexity and the period of treatment, which has been shortened from two years to six months; however, there is still more work to be done. Thus, the "focal point" in current TB drug development is to discover new drugs that have the capability to shorten and simplify the treatment programs. There is a need for more innovative and accurate, qualitative and quantitative bioanalytical methods for the use in pre-clinical and clinical drug development studies. Our research focused on one of the more promising antitubercular drug candidates in recent times, a nitroimidazole derivative known as TBA-354 which showed very promising results *in-vitro* and *in-vivo*.

We have developed and validated a liquid chromatography-tandem mass spectrometry (LC-MS/MS) method, for quantification of TBA-354, according to the EMA guidelines [1]. The method was utilized to evaluate the fundamental *in-vivo* pharmacokinetics and tissue distribution of the drug in a healthy rat model. As stated from the previous chapters, there is currently not a published validated LC-MS/MS method for quantification of TBA-354 in rat plasma, lung and brain samples. Biological samples have a high content of endogenous compounds such as proteins and lipids, which significantly affect the LC-MS/MS analysis, if not eliminated. Therefore, it was necessary to develop and optimize a modified-SPE extraction method for the isolation of the analyte of interest from the interfering compounds of the matrix, before LC-MS/MS analysis.

The pharmacokinetic and drug distribution study was conducted on healthy female Sprague-Dawley rats (weight of 120 ± 20 g) after intraperitoneal (i.p.) administration. The results obtained showed a similar pattern in the concentration-time profiles of the three biological samples (plasma, lungs and brain) where there was a gradual increase in drug absorption reaching the maximum concentration (C_{max}) after 6 h. However, the rates at the drug accumulated in the three biological matrices were not the same, the highest was in plasma followed by the lung and then the brain, respectively. The plasma to brain ratio was 32.89% at the T_{max} which reflects high blood-brain barrier (BBB) penetration of TBA-354. TBA-354 has a minimum inhibitory concentration (MIC) less than 0.36 µM (156.96 ng/mL) against ten different *Mycobacterium tuberculosis* (*M.tb*) strains and the C_{max} reached in the brain was 713.36 which is 4.54 times higher.

Studying the distribution of drugs in tissues is important in drug development, the evaluation of their localization at the target sites and understanding their toxic effects because of the accumulation. Recent improvements in mass spectrometry (MS) have led to the possibility of using matrix-assisted laser desorption/ionization (MALDI) mass spectrometry imaging (MSI) to visualize and map molecules directly from the biological tissue samples. Even though the MSI technique requires advanced and expensive analytical instrumentation, it is simple and when complemented with other advanced analytical methods such as LC-MS/MS, can provide invaluable information in drug development. The technique allows the direct evaluation of the spatial localization of both known and unknown compounds without any prior labeling. MSI can be customized to produce high-quality results while maintaining the spatial resolution of the target analytes. Our group has successfully used MSI in the past, to investigate the molecular histology of many different drugs and drug classes [2-7].

We have realized that the distribution of a drug in the brain tissue section is often non-uniform, thus concluding the study based on the results obtained from a single brain section is often not sufficient. Quantification of the total concentration of the drug in the brain using LC/MS/MS is necessary to support the spatial imaging results. Nevertheless, it is rational in a drug distribution study to expect the MSI results to be relative to the LC-MS/MS quantitative results, especially when investigating the time-dependent distribution of a drug. To support this statement, the MSI results were compared to the quantitative LC-MS/MS results of the same time points and they showed good correlation to each other.

The MSI results we obtained showed that the drug has a high BBB permeability and it accumulates in the neocortical regions of the brain and this explains the reason for the drug displaying certain neurotoxic signs during clinical trial as reported by the TB alliance [8]. The imaging experiments aided us in the understanding of the localization and accumulation of TBA-354 in different regions of the brain.

To conclude, this study has proven that LC-MS/MS is an accurate and highly sensitive technique that can be used in preclinical studies for quantification of TBA-354 in biological samples. The use of MSI in this study has provided the evidence as to why TBA-354 showed certain neurotoxic signs, during clinical trials. This demonstrates that in future drug development studies, LC-MS/MS and MSI techniques can be used complementarily for preclinical quantitative and drug distribution studies in the brain, thus allowing for a deeper understanding, and possibly predicting possible neurotoxic side effects

3.2. References

1. E.M.A. *European Medicines Agency, C.H.M.P. Committee for Medicinal Products for Human Use*, 2009. [cited 2016 15 March]; Available from: http://www.ema.europa.eu/docs/en_GB/document_library/Scientific_guideline/2011/08/WC500109686.pdf.
2. Baijnath, S., et al., *Evidence for the presence of clofazimine and its distribution in the healthy mouse brain.* Journal of Molecular Histology, 2015. **46**: p. 439-442.
3. Baijnath, S., et al., *Neuroprotective potential of Linezolid: a quantitative and distribution study via mass spectrometry.* Journal of Molecular Histology, 2016. **47**: p. 429-435.
4. Shobo, A., et al., *MALDI MSI and LC-MS/MS: Towards preclinical determination of the neurotoxic potential of fluoroquinolones.* Drug Testing and Analysis, 2015. **8**: p. 832-838.
5. Shobo, A., et al., *Visualization of Time-Dependent Distribution of Rifampicin in Rat Brain Using MALDI MSI and Quantitative LCMS/MS.* ASSAY and Drug Development Technologies, 2015. **13**: p. 277-284.
6. Shobo, A., et al., *Tissue distribution of pretomanid in rat brain via mass spectrometry imaging.* Xenobiotica, 2016. **46**: p. 247-252.
7. Munyeza, C.F., et al., *Rapid and widespread distribution of doxycycline in rat brain: a mass spectrometric imaging study.* Xenobiotica, 2016. **46**: p. 385-392.
8. i-Base. *The tuberculosis treatment pipeline: activity, but no answers*, 2016. [cited 2016 04 October]; Available from: http://i-base.info/htb/30164

Supporting information for chapter 2

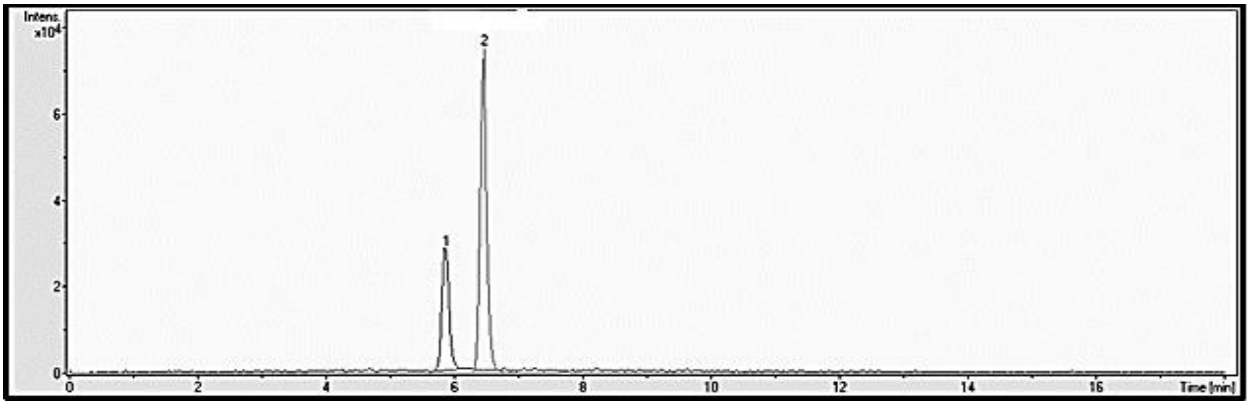

Figure S2.1. MRM chromatogram of (1) 250 ng/mL IS and (2) 500 ng/mL TBA-354 in rat plasma.

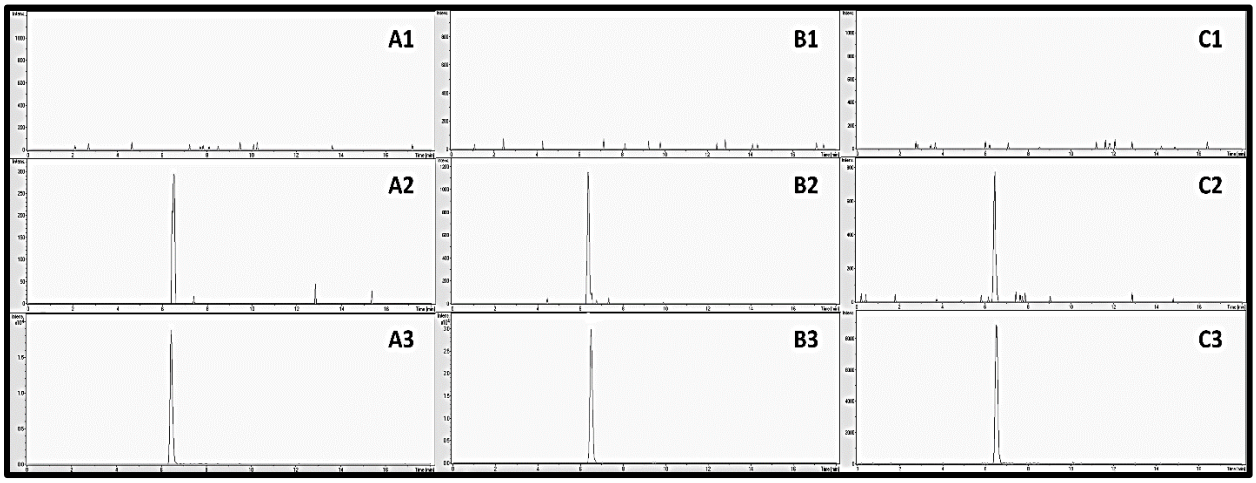

Figure S2.2. Representative MRM chromatograms for TBA-354 in rat plasma, lungs and brain homogenates. Blank plasma, lung and brain homogenates (A1, B1, and C1 respectively); blank plasma, lung and brain homogenates spiked with the analyte at LLOQ (A2, B2, and C2 respectively) and plasma and lung and brain homogenate samples obtained 6.00 h after i.p. injection (A3, B3, and C3).

Table S2.1. Extraction recoveries of TBA-354 using different SPE cartridges.

Matrix	Cartridge	% Recovery	% RSD
Plasma	HLB SPE (30 mg, 1 mL)	89.55	4.02
	HybridSPE-Phospholipid (30 mg, 1 mL)	107.20	3.70
	C_{18} (50 mg, 1 mL)	104.22	1.96
	C_{18} (100 mg, 1 mL)	97.70	3.82
Lungs	HLB SPE (30 mg, 1 mL)	105.13	2.03
	HybridSPE-Phospholipid (30 mg, 1 mL)	97.90	1.45
	C_{18} (50 mg, 1 mL)	109.07	4.78
	C_{18} (100 mg, 1 mL)	111.69	4.38
Brain	HLB SPE (30 mg, 1 mL)	96.37	2.56
	HybridSPE-Phospholipid (30 mg, 1 mL)	92.37	5.91
	C_{18} (50 mg, 1 mL)	107.90	9.35
	C_{18} (100 mg, 1 mL)	93.96	11.26